Fundamentals of magnetism

I.V. Bobkova

Contents

Chapter 1

Magnetism of atoms.

1.1 Mechanical and magnetic moment of an electron in an atomic orbit. Classical consideration.

If an electron moves in a circular orbit, then there is a certain relationship between its magnetic moment and angular momentum. Let $\boldsymbol{\mu}$ be the magnetic moment of the electron, and $\boldsymbol{J}$ its angular momentum. The vector $\boldsymbol{J}$ is directed perpendicular to the orbital plane and is equal in absolute value

$$J = mvr. \tag{1.1}$$

The magnetic moment of the same orbit is equal to the product of the current and the area of the orbit (in the SI system, in the CGS it must be divided by the speed of light). Current $I = q/(2\pi r/v)$, $S = \pi r^2$. Thus,

$$\mu = IS/c = qvr/2c. \tag{1.2}$$

The magnetic moment is also directed perpendicular to the

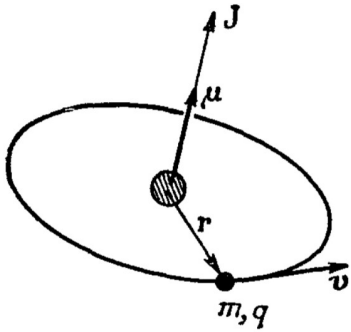

Figure 1.1: From [2]. Mechanical and magnetic moments of an electron moving in a circular orbit.

orbital plane. From Eqs.(1.1) and (1.2) we can obtain

$$\boldsymbol{\mu} = \frac{q}{2mc}\boldsymbol{J}. \tag{1.3}$$

Thus, the ratio of the magnetic moment of a moving charged particle to the mechanical one does not depend on either its speed or the radius of its orbit. In general, the ratio of the magnetic moment of a particle to its mechanical moment is called the gyromagnetic ratio. For an electron it is negative, because the electron has a negative charge.

1.2 Mechanical and magnetic moment of an electron in an atomic orbit. Quantum consideration.

If we consider the atomic nucleus to be infinitely heavy, then the Hamiltonian of an atom with Z spinless electrons takes

the form

$$\hat{H} = \sum_{i=1}^{Z}\Big(\frac{\hat{p}_i^2}{2m} - \frac{Ze^2}{r_i}\Big) + \sum_{i<j}\frac{e^2}{|r_i - r_j|}. \tag{1.4}$$

In a static magnetic field $\hat{p}_i \to \hat{p}_i - e\boldsymbol{A}(\boldsymbol{r}_i)/c$, where $\boldsymbol{A}(\boldsymbol{r})$ is the vector potential of the magnetic field. If the magnetic field is spatially homogeneous, then the vector potential can be chosen in the form $\boldsymbol{A}(\boldsymbol{r}) = (1/2)[\boldsymbol{B} \times \boldsymbol{r}]$. Then

$$(\boldsymbol{p} - \frac{e}{c}\boldsymbol{A})^2 = \hat{p}^2 - \frac{e}{c}(\boldsymbol{A}\hat{p} + \hat{p}\boldsymbol{A}) + \frac{e^2}{c^2}A^2 = \hat{p}^2 - \frac{e}{c}\boldsymbol{B}\hat{l} + \frac{e^2}{4c^2}B^2 r_\perp^2, \tag{1.5}$$

where $\hat{l} = \boldsymbol{r} \times \hat{p}$ is the angular momentum operator, and $r_\perp$ is the projection of $\boldsymbol{r}$ onto the plane perpendicular to $\boldsymbol{B}$. Then for the system of Z electrons in an atom we obtain

$$\hat{H} = \hat{H}_0 - \frac{e}{2mc}\boldsymbol{B}\hat{L} + \frac{e^2}{8mc^2}B^2\sum_{i=1}^{Z} r_{i\perp}^2, \tag{1.6}$$

where $\hat{L} = \sum\limits_{i=1}^{Z} \boldsymbol{r}_i \times \hat{p}_i$ is the operator of the total angular momentum of the Z electron system. For weak magnetic fields, the contribution of the third term can be neglected and the Hamiltonian of the system takes the form $\hat{H} = \hat{H}_0 - \boldsymbol{B}\boldsymbol{M}$, where $\boldsymbol{M} = \sum\limits_{i=1}^{Z} \boldsymbol{\mu}_i$ is the total magnetic moment of the electron system. Here the magnetic moment of an individual electron $\boldsymbol{\mu}_i$ is induced by its orbital moment as

$$\boldsymbol{\mu}_i = \frac{e}{2mc}\hat{\boldsymbol{l}}_i. \tag{1.7}$$

Thus, the gyromagnetic ratio in a quantum consideration of the orbital motion of an electron in an atom is obtained exactly the same as from an elementary classical consideration.

Let's direct the magnetic field along the z axis. Then the operators H_0, $\hat{L}^2$ and L_z have a common set of eigenvectors $|nLM\rangle$, and the eigenvalues of $\hat{H}_0$, E_0^{nL} do not depend on M and are $(2L+1)$-degenerate. The eigenvalue of the operator $\hat{H}$ corresponding to the eigenvector $|nLM\rangle$ is

$$E_{nLM} = E_0^{nL} - M\mu_B B, \tag{1.8}$$

where

$$\mu_B = \frac{e\hbar}{2mc}. \tag{1.9}$$

This quantity is called the Bohr magneton.

Because M can have all integer values from $-L$ to L, then in a magnetic field the level E_0^{nL} is split into $(2L+1)$ different equidistant levels (splits into a multiplet consisting of $(2L+1)$ sublevels). The distance between neighboring sublevels should be equal to $\mu_B B$ and should not depend on a particular atom. The splitting of atomic energy levels in a magnetic field is called the Zeeman effect.

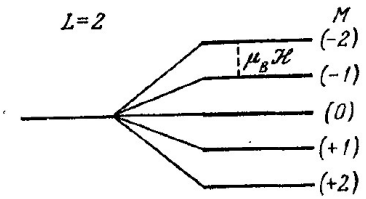

Figure 1.2: From [3]. Zeeman effect for $L = 2$. On the left is a degenerate energy level in a zero field, on the right is the splitting of this level in a non-zero magnetic field.

The experiment only partially confirms these predictions. There are 2 important deviations:

(1) in atoms with odd Z all multiplets are even, i.e. consist of an even number of sublevels. It looks like as if L is a half-integer.

(2) the distance between neighboring sublevels is equal to $g\mu_B B$, where g is the Lande-factor and depends on the specific multiplet.

1.3 The Stern-Gerlach experiment. Electron spin. Intrinsic magnetic moment of an electron.

To eliminate the difficulties described above, it is necessary to introduce half-integer angular momentum and a gyromagnetic ratio different from $e/2mc$. This is obtained if we introduce the electron spin hypothesis, put forward by Uhlenbeck and Goudsmit in 1925: each electron has an internal angular momentum or spin $s = (1/2)\hbar$, with which a magnetic moment is associated

$$\boldsymbol{\mu}_s = g_s \frac{e}{2mc} \boldsymbol{s}, \tag{1.10}$$

where g_s is some constant. Agreement between theory and experiment is achieved at $g_s = 2$. This value of g_s is derived from the nonrelativistic approximation of the Dirac equation.

The existence of a half-integer moment is directly established in the Stern-Gerlach experiment, which studies the deflection of a beam of atoms or molecules having a magnetic moment $\boldsymbol{\mu}$ in a nonuniform magnetic field. If the field is nonuniform, then the force $\boldsymbol{F} = \nabla(\boldsymbol{\mu B})$ acts on the center of mass of the atom. If an atom is in a state with a certain μ_z and the field gradient is directed along the z axis, see Fig. 1.3, then the average force acting on it is $\bar{F} = \mu_z dB/dz$.

Let l be the distance traveled by an atom in a magnetic field, T be the initial kinetic energy of the atom. Then the velocity of each atom deviates from its initial direction by an

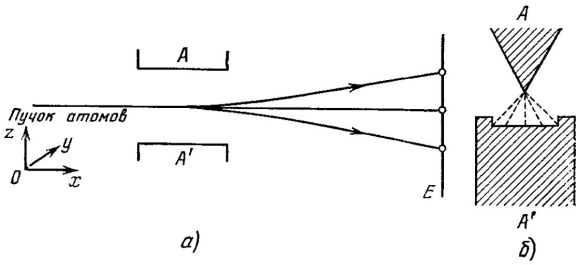

Figure 1.3: From [4]. The Stern-Gerlach experiment. (a) General experimental design. A non-uniform magnetic field acts between the poles of the magnet A and A' and is directed vertically; (b) Cross section of the poles of a magnet, the dotted lines indicate the magnetic field lines.

angle

$$\varphi \approx \mu_z \frac{dB_z}{dz} \frac{l}{2T}. \tag{1.11}$$

The deviation is proportional to μ_z. If the projection μ_z could take The spin magnetic moment of an electron is proportional to the electron's own angular momentum (spin) and is equal toarbitrary values, then a continuous spot elongated in the direction of the z axis would be observed on the screen. In fact, a number of discrete, equidistant spots are observed on the screen. When the field changes, the distance between the spots changes, but the total number of spots λ remains unchanged. Thus, this experiment is direct proof of the quantization of μ_z. Moreover, in the experiments of Stern and Gerlach with beams of silver atoms, splitting into 2 separate beams was obtained, which serves as proof of the half-integer value of the angular momentum of the corresponding atom.

A brief summary of the relationship between the magnetic and mechanical moment of an electron:

The magnetic moment of an electron consists of two sources:

orbital magnetism (due to motion in orbit) and spin magnetism

The orbital magnetic moment of an electron is proportional to the angular momentum of the electron due to its orbital motion and takes the form

$$\boldsymbol{\mu}_l = g_l \frac{\mu_B}{\hbar} \boldsymbol{l}, \tag{1.12}$$

where $g_l = 1$ - is the Lande-factor of the orbital motion.

The spin magnetic moment of an electron is proportional to the electron's own angular momentum (spin) and is equal to

$$\boldsymbol{\mu}_s = g_s \frac{\mu_B}{\hbar} \boldsymbol{s}, \tag{1.13}$$

where $g_s = 2$ - is the spin Lande-factor.

1.4 Electronic states in atoms.

The magnetic moment of an atom consists of the magnetic moments of its electron shell and the magnetic moment of the nucleus. The magnetic moment of a nucleus, in turn, consists of the magnetic moments of its constituent nucleons. Nucleons (protons and neutrons) also have a spin of $\hbar/2$ and an intrinsic magnetic moment of $\mu_p = g_p(e/2M_pc)s_p$ and $\mu_n = g_n(e/2M_nc)s_n$, respectively. $g_p \approx 5.59$ and $g_n \approx -3.83$ are the Lande spin factors of the proton and neutron. Although nuclear magnetism plays an important role in some effects, it is much weaker than electron magnetism (since Bohr's nuclear magneton $\mu_{nuc} = (e\hbar/2M_pc) \approx \mu_B/1836.5$) and in most magnetic materials, nanostructures and effects do not play a role, so we will focus on the magnetism of the electron shell of the atom. To do this, we first consider how the electronic states in an atom are arranged.

1.4.1 Energy levels of an atom of a given electronic configuration. Hund's rules.

Even for a given electronic configuration, an atom has several different states. As mentioned above, electrons in an atom move in the Coulomb field of the nucleus and interact with each other. In the nonrelativistic approximation, this interaction is purely electrostatic and does not depend on spin. The field is centrally symmetric, therefore the total orbital momentum of the electron system L is conserved, as well as the total spin of the electron system S. Thus, the degeneracy of each level is $(2L+1)(2S+1)$.

When taking into account relativistic effects, i.e. spin-orbit interaction $H_{so} \propto \boldsymbol{LS}$, the energy of the atom begins to depend not only on the values of L and S separately, but also on their mutual orientation. L and S are not conserved separately, but only the total momentum of the atom $\boldsymbol{J} = \boldsymbol{L} + \boldsymbol{S}$ is conserved. J can take values from $|L-S|$ to $L+S$, i.e. $2S+1$ values for $L > S$ and $2L+1$ values for $L < S$. At the same time, the spin-orbit interaction is usually weak, so because of it, a level with given L and S is usually split into very close sublevels, which are called the fine structure of the level. The atomic energy level (spectral term) is designated by the Latin letter S,P,D,F,G,H... according to the value of the total orbital momentum $L = 0, 1, 2, 3, ...$ The number $2S+1$ is placed at the top left - multiplicity; at the bottom right is J. For example, ${}^2P_{3/2}$ - atomic level $L = 1$, $S = 1/2$, $J = 3/2$.

There are empirically established Hund's rules, which determine the state of the atom with the lowest energy (ground state term) for a given electronic configuration, taking into account the Pauli principle:

1. For a given electronic configuration, the state with the highest S has the lowest energy.

2. For this S, the term with the largest L has the lowest

energy.

3. For given L and S, the state with the minimum possible $J = |L - S|$ has the lowest energy if the shell is less than half filled and with the maximum possible $J = L + S$ if the shell is more than half filled.

Let's look at examples.

Using Hund's rules, we determine the ground state term of the C and N atoms.

Carbon C. Electronic configuration $2s^2\ 2p^2$. The $2p$ shell is not completely filled. It has 2 electrons. By the first Hund rule $S = 1$, by the second Hund rule $L = 1$ ($L_z = 1 + 0 = 1$, this projection of the orbital momentum can correspond only to $L = 1$, and not to $L = 2$, since the action of the raising operator on this state leads to vanishing of the wave function due to the Pauli principle). The shell is less than half filled, so according to Hund's third rule $J = |L - S|$ =0. Ground state term $^3P_0$.

Nitrogen N. Electronic configuration $2s^2\ 2p^3$. The $2p$ shell is not completely filled. It has 3 electrons. According to the first Hund rule $S = 3/2$, according to the second Hund rule $L = 0$. The shell is exactly half filled, so $J = |L-S| = L+S = 3/2$. Ground state term $^4S_{3/2}$.

1.5 Magnetic moment of an atom. Lande-factor.

The resulting magnetic moment of the many-electron shell of the atom $\boldsymbol{\mu}$ will not be strictly opposite to the total orbital moment $\boldsymbol{J}$ due to the fact that the spin and orbital gyromagnetic ratios for the electron are different $g_l \neq g_s$. This is clear from Fig. 1.4, which represents a simplified vector model of the magnetic moment of an atom.

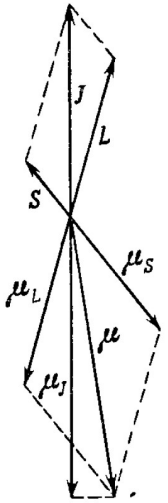

Figure 1.4: Vector model of the magnetic moment of an atom.

We are only interested in the projection of $\boldsymbol{\mu}$ onto the vector $\boldsymbol{J}$ ($\boldsymbol{\mu}_J$), because we consider states with a certain value of angular momentum.

$$\mu_J = \mu_S \cos(\boldsymbol{S}, \boldsymbol{J}) + \mu_L \cos(\boldsymbol{L}, \boldsymbol{J}). \tag{1.14}$$

$$\begin{aligned} \cos(\boldsymbol{S}, \boldsymbol{J}) &= \frac{S(S+1) + J(J+1) - L(L+1)}{2\sqrt{S(S+1)J(J+1)}}, \\ \cos(\boldsymbol{L}, \boldsymbol{J}) &= \frac{L(L+1) + J(J+1) - S(S+1)}{2\sqrt{L(L+1)J(J+1)}}, \end{aligned} \tag{1.15}$$

Substituting (1.15) into (1.14), and also taking into account that $\mu_L = \sqrt{L(L+1)}\mu_B$, $\mu_S = 2\sqrt{S(S+1)}\mu_B$, we get

$$\mu_J = \Big[1 + \frac{J(J+1) + S(S+1) - L(L+1)}{2J(J+1)}\Big] \sqrt{J(J+1)}\mu_B = g_J \sqrt{J(J+1)}\mu_B, \tag{1.16}$$

where

$$g_J = 1 + \frac{J(J+1) + S(S+1) - L(L+1)}{2J(J+1)} \tag{1.17}$$

This is the Lande factor of the electron shell. If $L = 0$ (pure spin magnetism), then $g_J = 2$. If $S = 0$ (pure orbital magnetism), then $g_J = 1$.

Quantum mechanical derivation of the Lande factor.

From symmetry considerations it is clear that, because in the absence of an external magnetic field, the only moment conserved in the system is the total moment $\boldsymbol{J}$, then the magnetic moment operator in the vector sense must be directed along $\boldsymbol{J}$. Therefore we can write

$$\hat{\boldsymbol{\mu}} = \hat{G}\hat{\boldsymbol{J}}, \tag{1.18}$$

where $\hat{G}$ is some scalar operator. By defining the magnetic moment as the sum of the orbital and spin moments, we obtain:

$$\hat{G}\hat{\boldsymbol{J}} = -\mu_B(\hat{\boldsymbol{L}} + 2\hat{\boldsymbol{S}}) = -\mu_B(\hat{\boldsymbol{J}} + \hat{\boldsymbol{S}}). \tag{1.19}$$

Multiplying this equality by $\hat{\boldsymbol{J}}$, we get:

$$\hat{G}\hat{\boldsymbol{J}}^2 = -\mu_B(\hat{\boldsymbol{J}}^2 + \hat{\boldsymbol{J}}\hat{\boldsymbol{S}}) = -\mu_B(\hat{\boldsymbol{J}}^2 + \hat{\boldsymbol{L}}\hat{\boldsymbol{S}} + \hat{\boldsymbol{S}}^2). \tag{1.20}$$

The operator $\hat{\boldsymbol{L}}\hat{\boldsymbol{S}}$ can be expressed from the relation:

$$\hat{\boldsymbol{J}}^2 = (\hat{\boldsymbol{L}} + \hat{\boldsymbol{S}})^2 = \hat{\boldsymbol{L}}^2 + 2\hat{\boldsymbol{L}}\hat{\boldsymbol{S}} + \hat{\boldsymbol{S}}^2. \tag{1.21}$$

As a result, from the equation (1.20) $\hat{G}$ can be expressed as

$$\hat{G} = -\mu_B\Big(1 + \frac{\hat{\boldsymbol{J}}^2 - \hat{\boldsymbol{L}}^2 + \hat{\boldsymbol{S}}^2}{2\hat{\boldsymbol{J}}^2}\Big). \tag{1.22}$$

And in a state with given S, L and J, all operators in this formula turn into their own values. That's why

$$\hat{\boldsymbol{\mu}} = -\mu_B\Big(1 + \frac{J(J+1) - L(L+1) + S(S+1)}{2J(J+1)}\Big)\hat{\boldsymbol{J}}. \quad (1.23)$$

Assuming the field is directed along z, from

$$\Delta E = -\langle\hat{\mu}_z\rangle B = g\mu_B m_J B, \quad (1.24)$$

where

$$g = 1 + \frac{J(J+1) - L(L+1) + S(S+1)}{2J(J+1)} \quad (1.25)$$

is the Lande-factor, and m_J is the projection of the total moment onto the z axis.

Chapter 2

Classification of materials according to their magnetic properties.

Phenomenological classification of magnetic materials is made according to their magnetic susceptibility. For most magnetic materials, the magnetization $\boldsymbol{M}$ in an external field $\boldsymbol{H}$ is parallel (or antiparallel) to the field and

$$\boldsymbol{M} = \chi \boldsymbol{H}, \tag{2.1}$$

where χ is the magnetic susceptibility. In a more general case, the magnetization can depend on the field in a nonlinear manner, then a differential susceptibility $\chi(H) = dM/dH$ can be introduced.

Based on different susceptibility behavior, three classes of magnetic materials can be distinguished:

1) diamagnets;

2) paramagnets;

3) materials with spontaneous magnetic order.

2.1 Diamagnetism.

Diamagnetism is a purely inductive effect. An external magnetic field induces magnetic dipoles in a material, which are oriented opposite to the external field in accordance with Lenz's rule. Therefore, the diamagnetic susceptibility is negative $\chi^{dia} < 0$.

Diamagnetism is a property of all materials. But it manifests itself experimentally only in the absence of paramagnetism and atomic magnetic order, which are much stronger and mask diamagnetic effects.

Examples of diamagnetic materials:

1) many organic compounds;

2) metals like Hg;

3) inert gases;

4) superconductors at $T < T_c$. They are ideal diamagnetic materials because for them, the external magnetic field is completely screened by the material (Meissner-Ochsenfeld effect). That is, $\chi = -1$ and $\boldsymbol{B} = \mu_0(\boldsymbol{H} + \boldsymbol{M}) = \mu_0(1 + \chi)\boldsymbol{H} = 0$.

2.2 Paramagnetism.

The susceptibility of paramagnetic materials is positive $\chi^{para} > 0$. A necessary condition for the occurrence of paramagnetism is the existence of permanent magnetic dipoles (except for Van Vleck polarization paramagnetism). In an external field, they are oriented along the field. This orientation is partially destroyed by thermal fluctuations. Permanent magnetic moments can be created by localized moments of the inner shells of an atom, or by collectivized conduction electrons.

Typical examples of materials where paramagnetism is created by localized moments of the inner shells of atoms are rare

earth metals, where magnetism is created by $4f$ electrons of the inner shells and $5f$ electrons in actinides. This class of materials exhibits Langevin paramagnetism, which is characterized by susceptibility behavior that obeys Curie's law

$$\chi^{Langevin}(T) = \frac{c}{T}. \tag{2.2}$$

Conductivity electrons also have a constant magnetic moment μ_B per electron. They also give the material a paramagnetic response to the field. This paramagnetism is called Pauli paramagnetism. The corresponding susceptibility is almost independent of the temperature $\partial\chi^{Pauli}/\partial T \approx 0$ and $\chi^{Pauli} \ll \chi^{Langevin}$.

2.3 Spontaneous magnetism.

This type of magnetism is caused by strong exchange interactions between atomic magnetic moments and can only be explained using quantum mechanics. Susceptibility can be highly dependent on temperature, external field, and sample history. Such materials are characterized by the presence of a critical temperature, below which the material exhibits spontaneous magnetization, not caused by an external field. This type of magnetism can be caused by both localized magnetic moments (Gd, EuO, EuS) and itinerant electrons (Fe, Ni, Co). The spontaneous magnetism can be roughly divided into three subclasses:

1) Ferromagnetism - there is spontaneous non-zero magnetization at $0 < T < T_c$ due to the preferable orientation of all atomic magnetic moments in one direction. T_c is called the Curie temperature.

2) Ferrimagnetism - the crystal lattice is divided into 2 sublattices A and B, in each of which the atoms are arranged

in a ferromagnetic order, but the magnetizations of these sublattices are not equal to each other $\boldsymbol{M}_A \neq \boldsymbol{M}_B$ and $\boldsymbol{M} = \boldsymbol{M}_A + \boldsymbol{M}_B \neq 0$ for $T < T_c$.

3) Antiferromagnetism is a special case of ferrimagnetism, for which $\boldsymbol{M}_A = -\boldsymbol{M}_B$ and, accordingly, $\boldsymbol{M} = \boldsymbol{M}_A + \boldsymbol{M}_B = 0$, i.e. there is no total magnetization, but each of the sublattices has non-zero spontaneous magnetization at $T < T_N$. In the case of antiferromagnetism, the critical temperature for the disappearance of spontaneous magnetic order T_N is called the Néel temperature.

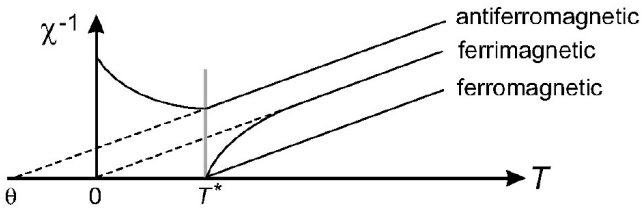

Figure 2.1: From [5]. Dependence of inverse magnetic susceptibility on temperature for materials with spontaneous magnetic order.

Above the critical temperature, all materials with spontaneous magnetic order exhibit paramagnetic properties. An approximate view of the dependence of magnetic susceptibility on temperature for all three types of materials with spontaneous order is presented in Fig. 2.1.

Chapter 3

Diamagnetism of systems of weakly interacting atoms or ions.

3.1 Classical consideration.

Let us assume that a magnetic field is turned on at the location of the atom. According to Faraday's law of electromagnetic induction, when the magnetic field changes, a vortex electric field will be generated, see Fig. 3.1.

$$2\pi r E = -\frac{d}{dt}(B\pi r^2) \Rightarrow E = -\frac{r}{2}\frac{dB}{dt}. \tag{3.1}$$

The induced electric field, acting on the electron, creates a torque eEr, which must be equal to the rate of change of angular momentum:

$$\frac{dJ}{dt} = -\frac{er^2}{2}\frac{dB}{dt}. \tag{3.2}$$

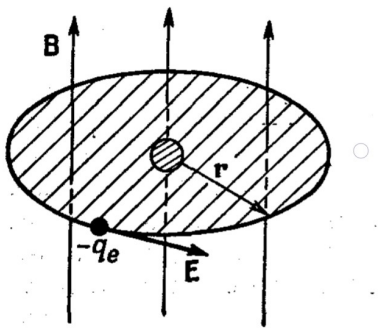

Figure 3.1: From [6]. An eddy electric field induced by an alternating magnetic field acting on an electron in an atom.

Integrating Eq. (3.2) over time, starting from $B = 0$ at $t = 0$, we obtain

$$\Delta J = -\frac{er^2}{2}B. \tag{3.3}$$

This additional angular momentum is transferred to the electron by turning on the field. The induced magnetic moment is obtained by multiplying the acquired orbital moment by the gyromagnetic ratio corresponding to the orbital motion

$$\Delta\mu = \frac{e}{2m}\Delta J = -\frac{e^2r^2}{4m}B. \tag{3.4}$$

The minus sign means that the induced magnetic moment is directed against the field, and this is diamagnetism. Susceptibility is equal to:

$$\chi^{dia} = -\frac{e^2r^2\mu_0}{4m}. \tag{3.5}$$

3.2 Quantum consideration.

The Hamiltonian of an atom without taking into account the spin of electrons in a magnetic field has the form (1.6). When

taking into account the electron spin, an additional term appears:

$$\hat{H} = \hat{H}_0 + \mu_B(g_L\hat{\boldsymbol{L}} + g_s\hat{\boldsymbol{S}})\boldsymbol{B} + \frac{e^2}{8mc^2}B^2\sum_{i=1}^{Z} r_{i\perp}^2, \qquad (3.6)$$

where $\hat{\boldsymbol{S}} = \sum_{i=1}^{Z} \hat{\boldsymbol{s}}_i$ is the operator of the total spin of electrons in an atom.

Let us consider an atom that has zero orbital and spin momentum, i.e. $L = S = 0$. Then the energy of the atom, which can be calculated as the average value of the operator $\hat{H}$ over a given quantum state, has the form:

$$E = E_0 + \frac{e^2}{8mc^2}B^2\langle 0|\sum_{i=1}^{Z}(x_i^2 + y_i^2)|0\rangle. \qquad (3.7)$$

Here the energy is calculated using perturbation theory. Eq. (3.7) is the result of a calculation accurate to the first order of perturbation theory in the magnetic field, therefore the averaging is taken not over the exact state in the magnetic field, but over the state $|0\rangle$, which corresponds to zero field.

Atoms and ions with a completely filled shell have a spherically symmetric wave function, so $\langle|x_i^2|\rangle = \langle|y_i^2|\rangle = (1/3)\langle|r_i^2|\rangle$.

$$\Delta E = E - E_0 = \frac{e^2B^2}{12mc^2}\langle 0|\sum_{i=1}^{Z} r_i^2|0\rangle. \qquad (3.8)$$

Magnetic moment per unit volume

$$M = -n\frac{\partial\Delta E}{\partial B} = -n\frac{e^2B}{6mc^2}\langle 0|\sum_{i=1}^{Z} r_i^2|0\rangle, \qquad (3.9)$$

where n is the concentration of atoms.

$$\chi^{dia} = -n\frac{e^2}{6mc^2}\langle 0|\sum_{i=1}^{Z} r_i^2|0\rangle. \qquad (3.10)$$

This is Larmor diamagnetic susceptibility. It does not depend on temperature, because the average square of the distance in a given state does not depend on temperature, and other states are usually quite strongly separated from a given one in energy and the energy of the thermal motion of surrounding particles is not enough to transfer a given atom to another state.

This diamagnetic susceptibility is very small and manifests itself directly mainly for atoms and ions with completely filled shells, although in fact it is inherent in absolutely all atoms. The fact is that atoms with partially filled shells have a permanent magnetic moment, due to which they exhibit paramagnetic properties. Therefore, diamagnetism is masked by a much larger paramagnetic contribution to the susceptibility. But for heavy atoms, in which the total spin moment does not exceed several Bohr magnetons, and the diamagnetic moments of all electrons add up, the diamagnetic contribution to the susceptibility can reach 10% of the total susceptibility, which is already significant.

3.3 Comparison with experiment.

If the atom's own magnetic moment is zero, then the diamagnetism of the electron shell comes to the fore. This applies primarily to inert gases and to vapor of elements of the second group, in which the ground state has the configuration ${}^1S_0$.

The susceptibility defined by the formula (3.10) is a dimensionless quantity. The so-called molar susceptibility, which is determined by the formula (3.10) with the atomic concentration n replaced by Avogadro's number N_A. This value, when multiplied by the magnetic field, gives the magnetic moment of a mole of the substance. It is no longer dimensionless and is expressed in cm^3/mol. A comparison of the molar suscepti-

bilities of inert gases with the calculation is given in the table in Fig. 3.2.

Element	He	Ne	Ar	Kr	Xe
$-\varkappa_{\text{a}} \cdot 10^6$, Experiment	1,9	6,7 ÷ 7,5	18 ÷ 19	28 ÷ 29	42 ÷ 44
$-\varkappa_{\text{a}} \cdot 10^6$, Theory	1,85	5,7	18,9	31,7	48,0

Figure 3.2: From [7]. Comparison of experimental results on the susceptibility of inert (noble) gases with calculations.

Negative halide ions and positive alkali metal ions have an electron shell similar to that of noble gases, so their susceptibilities can be expected to be close. The experimental ion susceptibilities are given in the table in Fig. 3.3.

Ion	$-\varkappa_{\text{и}} \cdot 10^6$	Atom	$-\varkappa_{\text{a}} \cdot 10^6$	Ion	$-\varkappa_{\text{и}} \cdot 10^6$
—	—	He	1,9	Li^+	1,0
F^-	9,1	Ne	7	Na^+	6,8
Cl^-	23,4	Ar	19	K^+	14,9
Br^-	35	Kr	28,5	Rb^+	22,5
J^-	50,6	Xe	43	Cs^+	35,0

Figure 3.3: From [7]. Comparison of molar susceptibilities of atoms and similar ions.

The susceptibilities of the corresponding ions and atoms are indeed close, but the susceptibility of halide ions is greater, and the susceptibility of alkali metal ions is less than that of noble gas atoms. This is due to the fact that the nuclear charge of halogens is less, and that of alkali metal ions is greater than that of atoms of inert gases; therefore, the orbital radii are greatest for halogens and least for alkali metals.

Chapter 4

Langevin paramagnetism.

4.1 Semiclassical consideration.

Let the magnetic field be directed along the z axis, i.e. $\boldsymbol{B} = (0, 0, B)$. The energy of interaction of the magnetic moment $\boldsymbol{\mu}$, directed at an angle θ to the z axis (more precisely, located in the angle range from θ to $\theta + d\theta$), with the magnetic field is

$$E = -\mu B \cos\theta. \tag{4.1}$$

the projection of the magnetic moment onto the z axis is equal to $\mu_z = \mu \cos\theta$. The probability of an atom having a magnetic moment in the angle range from θ to $\theta + d\theta$ is determined by the product of the Boltzmann distribution

$$P(\theta) = Ce^{\mu B \cos\theta/kT}. \tag{4.2}$$

to the fraction of states in which the magnetic moment lies in the angle range from θ to $\theta + d\theta$. This fraction is proportional to the spherical angle lying between the cones with openings θ and $\theta + d\theta$, i.e. $2\pi \sin\theta d\theta/4\pi$:

$$dw = \frac{1}{2} \sin\theta e^{\mu B \cos\theta/kT}. \tag{4.3}$$

Therefore, the average value of the projection of the magnetic moment onto the z axis is equal to

$$\langle \mu_z \rangle = \frac{\int \mu_z dw}{\int dw} = \frac{\int\limits_0^\pi \frac{1}{2}\mu \cos\theta \sin\theta e^{\mu B \cos\theta/kT} d\theta}{\int\limits_0^\pi \frac{1}{2} \sin\theta e^{\mu B \cos\theta/kT} d\theta}. \qquad (4.4)$$

Introducing the notations $\cos\theta = x$ and $(\mu B)/(kT) = y$, we obtain

$$\langle \mu_z \rangle = \mu \frac{\int\limits_{-1}^{1} x e^{xy} dx}{\int\limits_{-1}^{1} e^{xy} dx} = \mu[\coth y - \frac{1}{y}] = \mu L(y), \qquad (4.5)$$

where $L(y)$ is the Langevin function, which is shown in Fig. 4.1.

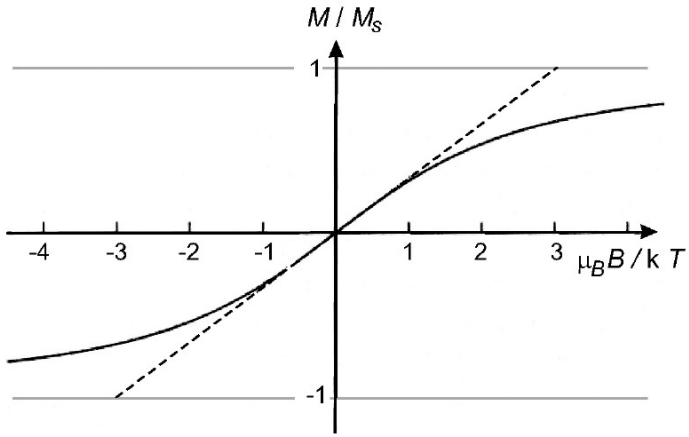

Figure 4.1: From [5]. Langevin function $L(\mu B/kT)$. The dotted line is the approximate linear behavior of the Langevin function $L(y) \approx y/3$ at $y \ll 1$.

Assuming that the external magnetic field is small or the temperature is high, i.e. $y \ll 1$, we can approximately write

$\coth y = 1/y + y/3 + O(y^3)$ and then

$$L(y) \approx \frac{y}{3}, \qquad y \ll 1. \tag{4.6}$$

Let n be the number of magnetic moments per unit volume, then the saturation magnetization is equal to $M_s = n\mu$. The average magnetization along the field takes the form

$$M = n\langle \mu_z \rangle. \tag{4.7}$$

At $\mu B/kT \ll 1$

$$\frac{M}{M_s} = \frac{\mu B}{3kT}, \tag{4.8}$$

then we obtain the susceptibility

$$\chi = \frac{M}{H} = \frac{\mu_0 \mu^2 n}{3k} \frac{1}{T} = \frac{C}{T}. \tag{4.9}$$

Thus, the paramagnetic susceptibility of a gas of non-interacting atoms obeys Curie's law.

4.2 Quantum consideration.

For a quantum calculation, it is necessary to take into account that the total angular momentum of a particle J can have integer or half-integer values. The energy of the magnetic moment in a magnetic field is $E = g_J m_J \mu_B B$. The average value of the projection of the magnetic moment onto the magnetic field axis can be calculated as the average over the Gibbs distribution for states with certain spin projections. First, we find the average value of the projection of the angular momentum:

$$\langle m_J \rangle = \frac{\sum\limits_{m_J=-J}^{J} m_J e^{-x m_J}}{\sum\limits_{m_J=-J}^{J} e^{-x m_J}} = -\frac{1}{Z} \frac{\partial Z}{\partial x}, \tag{4.10}$$

where $x = g_J\mu_B B/kT$. The magnetization per unit volume can then be expressed as:

$$M = -ng_J\mu_B\langle m_J\rangle. \tag{4.11}$$

Let's calculate the partition function:

$$Z = \sum_{m_J=-J}^{J} e^{-xm_J} = e^{Jx}\big(1 + e^{-x} + e^{-2x} + ... + e^{-2Jx}\big) = e^{Jx}\frac{1 - e^{-(2J+1)x}}{1 - e^{-x}} = \frac{e^{(2J+1)x/2} - e^{-(2J+1)x/2}}{e^{x/2} - e^{-x/2}} = \frac{\sinh[(2J+1)x/2]}{\sinh[x/2]}. \tag{4.12}$$

$$\frac{M}{M_s} = \frac{ng_J\mu\frac{1}{Z}\frac{\partial Z}{\partial x}}{ng_J\mu J} = \Big[\frac{2J+1}{2J}\coth[\frac{2J+1}{2J}y] - \frac{1}{2J}\coth[\frac{y}{2J}]\Big] = B_J(y), \tag{4.13}$$

where $y = Jx = g_J J\mu_B B/kT$ and $B_J(y)$ - is the Brillouin function, which is shown in Fig. 4.2 for different J.

Consider some limiting cases:

1. $J \to \infty$. In this case, for small x $\coth[y/2J] = \coth[x/2] \approx 2J/y + (1/3)(y/2J) + ...$ and for $B_J(y)$ we get

$$B_\infty(y) \approx \coth y - \frac{1}{y} - \frac{y}{12J^2} + ... \approx L(y). \tag{4.14}$$

This means that $J \to \infty$ corresponds to the classical limit.

2. $J = 1/2$. In this case

$$B_{1/2}(y) = \tanh y. \tag{4.15}$$

Now let's look at the typical experimental values $J = 1/2$, $g_J = 2$, $B = 1$T, $T = 300$K and estimate the characteristic

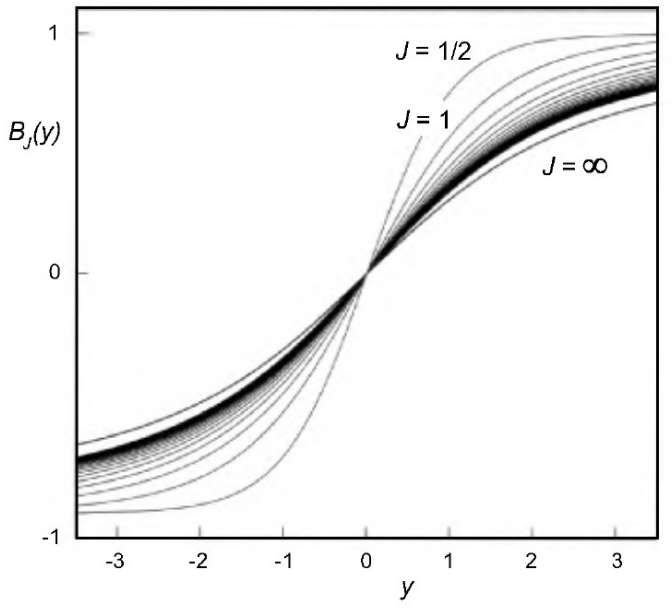

Figure 4.2: From [5]. Brillouin function for various values of J.

value y for these parameters $y = \mu_B B/kT \approx 2 \cdot 10^{-3} \ll 1$. Therefore, in most part of experimental situations $y \ll 1$ can be assumed, except in cases of very high fields or very low temperatures. In the case of $y \ll 1$ the Brillouin function can be simplified

$$B_J(y) \approx \frac{2J+1}{2J}\Big(\frac{2J}{2J+1}\frac{1}{y} + \frac{1}{3}\frac{2J+1}{2J}y\Big) - \frac{1}{2J}\Big(\frac{2J}{y} + \frac{y}{6J}\Big) = \frac{J+1}{3J}y. \tag{4.16}$$

Susceptibility is equal to

$$\chi = \frac{M}{H} = \frac{\mu_0 M_s B_J(y)}{B} = \frac{\mu_0 n g_J \mu_B J(J+1) g_J J \mu_B}{3JkT} = \frac{\mu_0 n g_J^2 \mu_B^2 J(J+1)}{3kT} = \frac{n\mu_0 \mu_{eff}^2}{3kT}. \tag{4.17}$$

Comparing the expression (4.17) with the classical answer for susceptibility (4.9), we see that they coincide up to the replacement $\mu \to \mu_{eff} = g_J \mu_B \sqrt{J(J+1)}$. Please note that in this case the saturation magnetization is achieved not by multiplying μ_{eff} by the number of moments per unit volume, but as $M_s = n g_J \mu_B J$.

4.3 Comparison with experiment. Alkali metal vapors. Salts of rare earth elements.

The number of possible substances where the law (4.17) is implemented is small, because Most gases have polyatomic molecules. Only inert gases and metal vapors are monatomic. The intrinsic magnetic moment of atoms of noble gases is zero, so only vapors of metals are suitable for observation.

Experiments were carried out with potassium vapor at $T = 600 - 800$K. It turned out that $\chi_K = 0.38/T$ (per mole). The theoretical value calculated using Eq. (4.17) gives fairly good agreement with experiment.

In addition to metal vapors, salts of rare earth elements are suitable objects in which Langevin paramagnetism can be observed. For rare earth elements, the inner $4f$ shell is underfilled, see the table in Fig. 4.3. The magnetic moment is created by this underfilled shell and this shell is well shielded from the influence of the electric fields of neighboring atoms by the filled $5s$ and $5p$ shells. Therefore, salts of rare earth elements can indeed be considered a gas of independent magnetic moments.

From a comparison of the experimental data presented in the table in Fig. 4.3 with calculations using the Hund formula (4.17) it is clear that the agreement is generally good, except

Ion	Number of 4f-electrons	Ground state term	S	L	J	g	μ/μ_B Hund	μ/μ_B Van Vleck	μ/μ_B exp.
La^{3+}	0	$^1S_0$	0	0	0	—	0	0	0
Ce^{3+}	1	$^2F_{5/2}$	1/2	3	5/2	6/7	2,54	2,56	2,4
Pr^{3+}	2	$^3H_4$	1	5	4	4/5	3,58	3,62	3,5
Nd^{3+}	3	$^4J_{9/2}$	3/2	6	9/2	8,11	3,62	3,68	3,5
Pm^{3+}	4	$^5J_4$	2	6	4	3/5	2,68	2,83	—
Sm^{3+}	5	$^6H_{5/2}$	5/2	5	5/2	2/7	0,84	1,6	1,5
Eu^{3+}	6	$^7F_0$	3	3	0	—	0	3,45	3,6
Gd^{3+}	7	$^8S_{7/2}$	7/2	0	7/2	2	7,94	7,94	8,0
Tb^{3+}	8	$^7F_6$	3	3	6	3/2	9,72	9,7	9,5
Dy^{3+}	9	$^6H_{15/2}$	5/2	5	15/2	4/3	10,65	10,6	10,7
Ho^{3+}	10	$^5J_8$	2	6	8	5/4	10,61	10,6	10,3
Er^{3+}	11	$^4J_{15/2}$	3/2	6	15/2	6/5	9,58	9,6	9,5
Tu^{3+}	12	$^3H_6$	1	5	6	7/6	7,56	7,6	7,3
Yb^{3+}	13	$^7F_{7/2}$	1/2	3	7/2	8/7	4,54	4,5	4,5
Lu^{3+}	14	$^1S_0$	0	0	0	—	0	0	0

Figure 4.3: From [7]. Effective magnetic moments of rare earth ions calculated using Hund's formula (4.17), Van Vleck's formula (4.18) and experimental value.

for Sm^{3+} and Eu^{3+} ions, for which there is a large discrepancy. This is because the derivation of (4.17) assumed that all ions are in their ground state. But they also have higher energy states (see Fig. 4.4), into which some of the ions can move at finite temperatures in accordance with the Boltzmann distribution $e^{-\varepsilon/kT}$. As can be seen from the figure, for samarium and europium the probability of the ion being in excited states at room temperature is not small, in contrast to other ions, for which the excited states are separated from the ground state by a large energy gap. Magnetic susceptibility, taking into account the excited states of ions, can be calculated using the

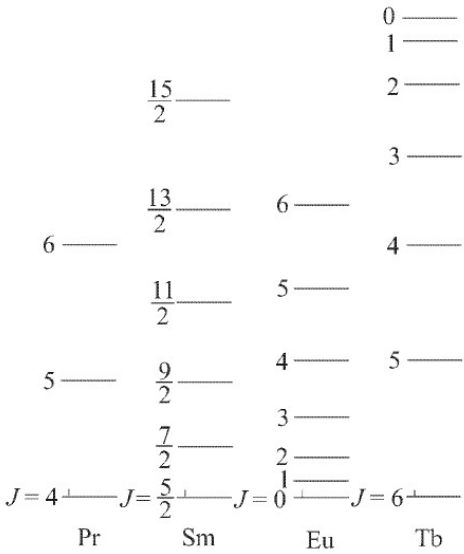

Figure 4.4: From [7]. Diagrams of the energy levels of some rare earth ions.

Van Vleck formula:

$$\chi = n \frac{\sum_J \left\{ g_J^2 \mu_B^2 J(J+1)/3kT + b_J \right\} (2J+1) e^{-\varepsilon_J/kT}}{\sum_J (2J+1) e^{-\varepsilon_J/kT}}. \quad (4.18)$$

Thermal excitation of atoms and molecules is only one of the reasons leading to deviations from Hund's formula (4.17). Other reasons include the intracrystalline Stark effect, which will now be briefly discussed, the electrostatic exchange interaction of electrons, which in some cases leads to ferromagnetism and will be discussed in detail later, and the magnetic interaction between the magnetic moments of individual atoms, which is significant only at very low temperatures.

In addition to rare earth elements, there are 4 more groups of elements in the periodic table in which the internal shells

are refilled. This

1) group of iron from Sc(Z=21) to Ni(Z=28) - the $3d$-shell is filled;

2) palladium group from Y(Z=39) to Pd(Z=46) - the $4d$ shell is filled;

3) platinum group from Lu(Z=71) to Pt(Z=78) - the $5d$ shell is filled;

4) group of actinides from Ra (Z=88) to Md (Z=101) - the $6d$ shell is filled first, and then the $5f$ shell.

Transition elements are the groups of iron, palladium and platinum in which the d-shells are filled. It would seem that their magnetic properties should be determined by the magnetic moment of the unfilled d-shell and the susceptibility should be calculated using the Hund or Van Vleck formulas. But it is not so. The effective magnetic moment calculated using Hund's formula for these materials is consistent with experiment only if the ground state of the atom is the S-state with zero orbital momentum. For most transition elements, the calculation can be consistent with experiment, if we assume that only the spin of the atom is oriented in the magnetic field, the susceptibility is calculated using the formula (Stoner's formula)

$$\chi = n\frac{4S(S+1)\mu_B^2}{3kT}, \tag{4.19}$$

that is, the effective magnetic moment is of purely spin nature $\mu_{eff} = 2\sqrt{S(S+1)}\mu_B$. The orbital angular momentum is frozen and does not participate in the orientation of the magnetic moment along the field, and therefore does not contribute to the susceptibility. The freezing of the orbital momentum occurs under the influence of the electric field of neighboring ions of the crystal lattice, which removes the degeneracy of energy levels in m_l. This is called the crystalline Stark effect. For transition element ions, unlike rare earth ions, the unfilled d-

shell is located on the outside, so the influence of the crystal field in their case is large.

Chapter 5

Magnetism of a free electron gas.

5.1 Fermi gas of non-interacting electrons.

5.1.1 Ground state of electron Fermi gas.

Let us consider a system of N non-interacting electrons located in volume V. Because electrons do not interact, it is enough to calculate the energy levels of one electron and fill them with electrons in accordance with the Pauli principle.

In the absence of interaction, the one-electron wave function satisfies the Schrödinger equation

$$-\frac{\hbar^2}{2m}\left(\frac{\partial^2}{\partial x^2}+\frac{\partial^2}{\partial y^2}+\frac{\partial^2}{\partial z^2}\right)\psi(\boldsymbol{r})=\varepsilon\psi(\boldsymbol{r}). \tag{5.1}$$

The movement of electrons is restricted by the volume V of the metal. For sufficiently large volumes, it is natural to expect that the bulk properties of the electron gas will not depend on the specific shape of the surface. Therefore, for simplicity, we

choose a cubic sample with side $L = V^{1/3}$ and impose periodic boundary conditions

$$\begin{aligned} \psi(x, y, z + L) &= \psi(x, y, z) \\ \psi(x, y + L, z) &= \psi(x, y, z) \\ \psi(x + L, y, z) &= \psi(x, y, z). \end{aligned} \tag{5.2}$$

The solution of the Schrödinger equation (5.1) has the form

$$\psi(\boldsymbol{r}) = \frac{1}{\sqrt{V}} e^{i\boldsymbol{k}\boldsymbol{r}}, \tag{5.3}$$

where the normalization factor $1/\sqrt{V}$ is chosen so that the total probability of finding an electron anywhere in the volume V is equal to unity $\int dV |\psi(\boldsymbol{r})|^2 = 1$. In this case $\varepsilon(\boldsymbol{k}) = k^2/2m$. Obviously, the solution (5.3) is an eigenfunction of the momentum operator corresponding to the eigenvalue $\hbar\boldsymbol{k}$. Therefore, this solution represents a state with a certain momentum $\hbar\boldsymbol{k}$ and velocity $\boldsymbol{v} = \hbar\boldsymbol{k}/m$.

The wave function (5.3) satisfies the boundary conditions (5.2) only if the following relations are satisfied:

$$\begin{gathered} e^{ik_x L} = e^{ik_y L} = e^{ik_z L} = 1 \Rightarrow \\ k_x = \frac{2\pi n_x}{L}, k_y = \frac{2\pi n_y}{L}, k_z = \frac{2\pi n_z}{L}, \end{gathered} \tag{5.4}$$

where n_x, n_y, n_z - are integer numbers. Thus, in k-space only such wave vectors are allowed whose coordinates along three axes are integer multiples of $2\pi/L$, see Fig. 5.1.

In the three-dimensional case, the volume region Ω in k-space contains $N_{k,V}$ points:

$$N_{k,V} = \frac{\Omega}{(2\pi/L)^3} = \frac{\Omega V}{(2\pi)^3}. \tag{5.5}$$

The level density in k-space is equal to

$$N_k = \frac{V}{(2\pi)^3}. \tag{5.6}$$

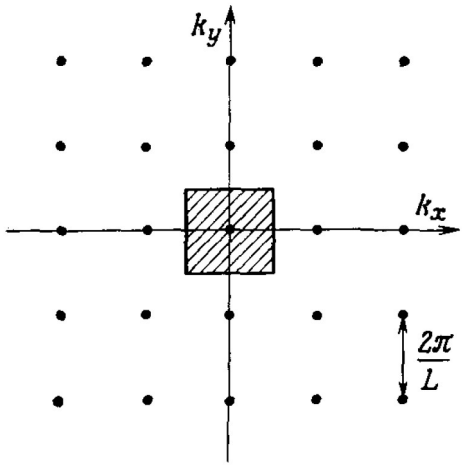

Figure 5.1: From [?]. Points of two-dimensional k-space having coordinates $k_x = 2\pi n_x/L$, $k_y = 2\pi n_y/L$. There is a shaded volume of $(2\pi/L)^2$ per point.

We will fill states in k-space with electrons taking into account the Pauli exclusion principle, i.e. in a state with a given $\boldsymbol{k}$, no more than 2 electrons with opposite spin projections on the quantization axis can be placed. The N-electron state is a filled sphere in k-space. Let the radius of this sphere be k_F. Then inside the filled sphere there is

$$\frac{V}{(2\pi)^3}\frac{4\pi k_F^3}{3} \tag{5.7}$$

states, in each of which two electrons can be placed. Therefore, the Fermi radius k_F is related to the total number of electrons in the system by the relation

$$N = 2\frac{V}{(2\pi)^3}\frac{4\pi k_F^3}{3} = \frac{k_F^3}{3\pi^2}V. \tag{5.8}$$

Thus, if the electron concentration in the system is n, then the ground state of the electron gas is obtained by filling all one-electron states up to the Fermi momentum $p_F = \hbar k_F$, which

is determined from the relation

$$n = \frac{k_F^3}{3\pi^2}. \tag{5.9}$$

States with momenta above p_F remain unoccupied.

A sphere with radius k_F, inside which filled electronic levels lie, is called the Fermi sphere, the surface of this sphere is called the Fermi surface. $v_F = p_F/m$ and $\varepsilon_F = p_F^2/2m$ are the Fermi velocity and Fermi energy, respectively. The Fermi velocity is the characteristic velocity of electrons in metals and is an analogue of the thermal velocity $v = \sqrt{3kT/m}$ in classical gases.

The order of magnitude of the Fermi velocity is $10^8 cm/s$. This is quite a high speed, about 1% of the speed of light. From the point of view of classical physics, such electron velocities look strange, because we describe the state of the system at $T = 0$, and at zero temperature in a classical gas all particles have zero velocities. Even at room temperature, the characteristic velocities of classical particles with the mass of an electron are only about $10^7 cm/s$.

The Fermi energy is on the order of several electronvolts.

Let us find the energy of the ground state of the Fermi gas. To do this, we need to add up the energies of all one-electron levels located inside the Fermi sphere:

$$E = 2\sum_{k<k_F} \frac{\hbar^2 k^2}{2m} = \frac{V}{(2\pi)^3}\sum_k \frac{\hbar^2 k^2}{2m}\Delta k = 2V\int \frac{d^3k}{(2\pi)^3}\frac{\hbar^2 k^2}{2m}. \tag{5.10}$$

$$E = 2V\int \frac{d^3k}{(2\pi)^3}\frac{\hbar^2 k^2}{2m} = \frac{V}{\pi^2}\int_0^{k_F} k^2 dk \frac{\hbar^2 k^2}{2m} = \frac{V}{10\pi^2}\frac{\hbar^2}{m}k_F^5. \tag{5.11}$$

Ground state energy per 1 electron

$$\frac{E}{N} = \frac{1/(10\pi^2)(\hbar^2/m)k_F^5}{k_F^3/3\pi^2} = \frac{3}{5}\varepsilon_F = \frac{3}{5}kT_F. \tag{5.12}$$

In a classical electron gas at $T = 0$ $E/N = 0$, and the energy $(3/5)\varepsilon_F$ is achieved at $T \sim 10^4 K$.

Note that we considered the Fermi energy of the gas as the product of the energy $\varepsilon_k = \hbar^2 k^2/2m$ of one state with a given $\boldsymbol{k}$ by the number of states in a small volume of k-space. Because the energy ε_k depends only on the modulus k, then we can proceed to integration over k, and hence to integration over the energy ε. It's done like this

$$\frac{d^3k}{(2\pi)^3} = \frac{4\pi k^2 dk}{(2\pi)^3} = g(\varepsilon)d\varepsilon,$$

$$g(\varepsilon) = \frac{m}{2\hbar^2\pi^2}\sqrt{\frac{2m\varepsilon}{\hbar^2}} = \frac{3}{4}\frac{n}{\varepsilon_F}\Big(\frac{\varepsilon}{\varepsilon_F}\Big)^{1/2}. \tag{5.13}$$

The quantity $g(\varepsilon)$ is called the energy density of states. Using the density of states, the expression for the Fermi energy of a gas can be written as

$$E = 2\int_0^{\varepsilon_F} \varepsilon d\varepsilon g(\varepsilon). \tag{5.14}$$

5.1.2 Fermi gas at finite temperatures.

The previous consideration is valid for $T = 0$. At $T > 0$, the density of states remains unchanged, and the probability of levels being occupied by electrons (distribution function) changes and is expressed by the Fermi function

$$f(\varepsilon) = \frac{1}{e^{(\varepsilon-\mu)/kT} + 1}. \tag{5.15}$$

At $T = 0$

$$f(\varepsilon) = \begin{cases} 0, & \varepsilon > \mu, \\ 1, & \varepsilon < \mu. \end{cases} \tag{5.16}$$

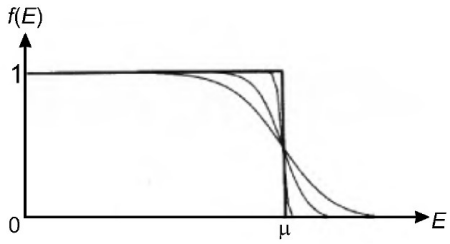

Figure 5.2: Fermi distribution.

Thus, at $T = 0$ $\varepsilon_F = \mu$. At non-zero temperatures, the step in the Fermi function smears, see Fig. 5.2. The width of the temperature smeared region is $\sim kT$. In addition, at non-zero temperatures the equality $\varepsilon_F = \mu$ is violated. The Fermi energy does not depend on temperature; it is a characteristic of the ground state of the Fermi gas, which is determined only by the electron density. And chemical potential depends on temperature. At low temperatures, this dependence has the form $\mu = \varepsilon_F - (\pi^2/6)(kT)^2(g'(\varepsilon_F)/g(\varepsilon_F))$, where $g'(\varepsilon_F)$ is the derivative of the density of states with respect to energy, taken at the Fermi energy. The order of magnitude of the correction to the chemical potential at low temperatures is $\Delta\mu/\mu \sim (kT/\varepsilon_F)^2$, which is approximately 10^{-2} at room temperature. At very high temperatures $T > T_F$ the chemical potential becomes negative. Under the condition $e^{-\mu/kT} \gg 1$, the occupation numbers of fermion states $f(\varepsilon)$ become small for any positive energy value and the Fermi-Dirac distribution transforms into the Boltzmann distribution.

At non-zero temperatures, the Fermi energy of the gas must be calculated taking into account the distribution function

$$E = \int_0^\infty \varepsilon d\varepsilon g(\varepsilon) f(\varepsilon). \tag{5.17}$$

Note that at $T = 0$ Eq. (5.17) becomes (5.14).

5.2 Pauli paramagnetism.

Let us calculate the magnetic moment of the Fermi gas. The magnetic moment of a unit volume can be calculated as the product of the magnetic moment of one electron and the difference in the concentrations of electrons with a magnetic moment along and against the field

$$M = \mu_B(n_\uparrow - n_\downarrow). \tag{5.18}$$

The electron concentration $n_{\uparrow,\downarrow}$ can be calculated similarly to the Fermi energy of a gas through the density of states and the distribution function

$$n_{\uparrow,\downarrow} = \int_0^\infty d\varepsilon g_{\uparrow,\downarrow}(\varepsilon) f(\varepsilon). \tag{5.19}$$

Next, we should take into account that in the presence of a magnetic field, the total energy of the electron consists not only of the kinetic energy $\varepsilon_k = k^2/2m$, but also the potential energy $\mp\mu_B B$, i.e. $\varepsilon_{\uparrow,\downarrow} = \varepsilon_k \mp \mu_B B$. Therefore, the density of states is now split along the spin: for the magnetic moment $\uparrow$ goes down by $-\mu_B B$, and for the magnetic moment $\downarrow$ goes up by the same amount, see Fig. 5.3.

Now the density of states $g_{\uparrow,\downarrow}(\varepsilon) = g_(\varepsilon \pm \mu_B B)$, where $g(\varepsilon)$ is expressed by the formula (5.13). For $\mu_B B \ll kT$ we can write $g_{\uparrow,\downarrow}(\varepsilon) \approx g(\varepsilon) \pm \mu_B B g'(\varepsilon)$. Then from (5.18) and (5.19) we get

$$M = 2\mu_B^2 B \int g'(\varepsilon) f(\varepsilon) d\varepsilon = -2\mu_B^2 B \int g(\varepsilon) f'(\varepsilon) d\varepsilon. \tag{5.20}$$

For $T \ll \varepsilon_F$ $f'(\varepsilon) \approx -\delta(\varepsilon - \varepsilon_F)$. That's why

$$M = 2\mu_B^2 B g(\varepsilon_F). \tag{5.21}$$

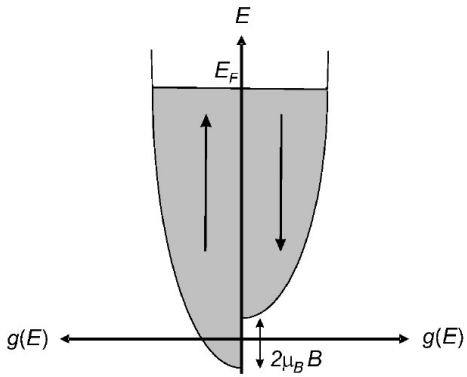

Figure 5.3: Spin splitting of the density of states for a Fermi gas in a magnetic field.

The magnetic susceptibility of the Fermi gas takes the form

$$\chi^{Pauli} = \frac{\mu_0 M}{B} = 2\mu_0 \mu_B^2 g(\varepsilon_F) = \frac{3n\mu_0\mu_B^2}{2\varepsilon_F}. \qquad (5.22)$$

This result depends very weakly on temperature and works well even for room temperatures. The temperature correction to the Pauli susceptibility is again of the order of magnitude $(kT/\varepsilon_F)^2$. Comparing the expression (5.22) with the Langevin susceptibility $\chi^{para} = n\mu^2/3kT$, we see that $\chi^{Pauli}/\chi^{para} \sim kT/\varepsilon_F$. The physical explanation of this fact is that, due to the Pauli principle, in a Fermi gas, not all electrons tend to line up along the field, but only those sitting at a distance $\sim kT$ from the Fermi energy, because only there are free places in the density of states with opposite spin. Such electrons exhibit standard Langevin paramagnetism, but their fraction is only kT/ε_F. That is, the Pauli principle suppresses the desire of electrons to line up in the field much more effectively than temperature.

5.3 Landau diamagnetism.

5.3.1 Landau quantization.

Let us consider a gas of non-interacting electrons in an external magnetic field $\boldsymbol{B} = B\boldsymbol{e}_z$. Then the vector potential of such a field can be chosen in the form $\boldsymbol{A} = (-By, 0, 0)$. In the presence of a vector potential, the electron momentum operator is replaced by $\hat{\boldsymbol{p}} \to \hat{\boldsymbol{p}} - (e/c)\boldsymbol{A}$. The Hamiltonian of the electron gas takes the form:

$$\hat{H} = \frac{1}{2m}\Big(\hat{p}_x + \frac{eBy}{c}\Big)^2 + \frac{\hat{p}_y^2}{2m} + \frac{\hat{p}_z^2}{2m} + g\mu_B \hat{s}_z B. \qquad (5.23)$$

The operator $\hat{s}_z$ commutes with the Hamiltonian, i.e. $[\hat{H}, \hat{s}_z] = 0$, therefore s_z is preserved in this state and the operator term in the Hamiltonian $-g\mu_B \hat{s}_z B$ can be replaced by the number $-g\mu_B s_z B$, if we consider only electronic states with a certain $s_z = \pm 1/2$. Then the electron wave function $\psi(\boldsymbol{r}, s_z)$ obeys the Schrödinger equation

$$\frac{1}{2m}\Big[\Big(\hat{p}_x + \frac{eBy}{c}\Big)^2 + p_y^2 + \hat{p}_z^2\Big]\psi + g\mu_B s_z B\psi = E\psi. \qquad (5.24)$$

Because the Hamiltonian does not depend on the coordinates x, z, then in these directions the wave function has the form of a plane wave and the solution of Eq. (5.24) can be found in the form:

$$\psi = e^{i(p_x x + p_z z)/\hbar}\varphi(y). \qquad (5.25)$$

Substituting (5.25) into (5.24), we obtain a one-dimensional equation for the function $\varphi(y)$, which can be written as:

$$\varphi'' + \frac{2m}{\hbar^2}\Big[\big(E - g\mu_B s_z B - \frac{p_z^2}{2m}\big) - \frac{m}{2}\omega_B^2 (y - y_0)^2\Big]\varphi = 0, \qquad (5.26)$$

where $\omega_B = eB/mc$ is the cyclotron frequency and $y_0 = -cp_x/(eB)$. Equation (5.26) is the equation of a harmonic

oscillator, so the energies of the stationary states of this equation have the form:

$$E_n = \hbar\omega_B(n+\frac{1}{2}) + g\mu_B s_z B + \frac{p_z^2}{2m} = \hbar\omega_B(n+\frac{1}{2}+\frac{g}{2}s_z) + \frac{p_z^2}{2m}. \quad (5.27)$$

The corresponding wave functions of stationary states have the form:

$$\varphi_n = \frac{1}{\pi^{1/4}x_0^{1/4}\sqrt{2^n n!}} \exp\Big(-\frac{(y-y_0)^2}{2x_0}\Big) H_n\Big(\frac{y-y_0}{x_0}\Big), \quad (5.28)$$

where $x_0 = \sqrt{\hbar/m\omega_B}$. From (5.28) it is clear that y_0 has the value of the y-coordinate of the center of the classical circle along which the electron moves in a magnetic field.

Any values of p_x correspond to a given Landau level E_n, so formally the Landau level is infinitely degenerate. In fact, the degeneracy of Landau levels is large, but not infinite. Let's find it. Let the sample have dimensions L_x and L_y in a plane perpendicular to the magnetic field. Then the number of allowed values of the x-component of the electron momentum lying in the interval Δp_x has the form:

$$N_{p_x} = \frac{L_x \Delta p_x}{2\pi\hbar}. \quad (5.29)$$

The y-coordinate of the center of the electron orbit must fall inside the sample, so $0 < y_0 < L_y \Longrightarrow \Delta p_x = eBL_y/c$. Then from (5.29) we get:

$$N_{p_x} = \frac{eB}{2\pi\hbar c} L_x L_y. \quad (5.30)$$

One can also calculate the number of Landau levels per interval of values of the z-momentum component Δp_z:

$$N_{p_x,p_z} = \frac{eBL_xL_y}{2\pi\hbar c}\frac{L_z\Delta p_z}{2\pi\hbar} = \frac{eBV}{(2\pi\hbar)^2 c}\Delta p_z. \quad (5.31)$$

5.3.2 Landau diamagnetism.

As we know, the magnetic moment of any classical system of charges in equilibrium is zero. In 1930, Landau showed that an electron gas has a diamagnetic moment even in the case of Boltzmann statistics. The point here is precisely the emergence of quantized stationary states of electron gas in a magnetic field, which were discussed in the previous section. Let's find this diamagnetic moment.

In the case of Boltzmann statistics, the average magnetic moment of the system can be found as

$$\langle \mu \rangle = \Big[\sum_l \mu_l g_l e^{-E_l/kT} \Big] / \Big[\sum_l g_l e^{-E_l/kT} \Big], \tag{5.32}$$

where μ_l is the magnetic moment of the system in a given state l, g_l is the number of states with a given energy E_l. Taking into account the fact that the energy of the system in a magnetic field depends on the magnetic moment as $E_l = E_{l,0} - \boldsymbol{\mu}_l \boldsymbol{B}$, we can write that

$$\langle \mu \rangle = kT \frac{dZ/d\boldsymbol{B}}{Z}, \tag{5.33}$$

where $Z = \sum\limits_l g_l \exp[-E_l/kT]$ is the partition function of the system. Then the average magnetic moment per unit volume of the system is

$$\boldsymbol{M} = nkT \frac{dZ/d\boldsymbol{B}}{Z}, \tag{5.34}$$

where n is the electron concentration.

Let us find the partition function for a gas of non-interacting charged particles obeying Boltzmann statistics:

$$Z = \sum_{\nu=0}^{\infty} \int\limits_{-\infty}^{\infty} dp_z \frac{2eBV}{(2\pi\hbar)^2 c} e^{-[\mu_B B(2\nu+1)/kT + p_z^2/2mkT]}. \tag{5.35}$$

Here we used the number of Landau levels (5.31) per interval of values of the z-momentum component Δp_z. The origin of the factor 2 is due to the fact that for free electrons $g = 2$ and then the spectrum of Landau levels has an additional twofold degeneracy in the electron spin: $E_n(s_z = 1/2) = E_{n+1}(s_z = -1/2)$.

Calculating the integral over p_z in (5.35), we obtain:

$$Z = \frac{2eBV}{(2\pi\hbar)^2 c}\sqrt{2mkT\pi}\sum_{\nu=0}^{\infty} e^{-\mu_B B(2\nu+1)/kT} = \frac{eBV}{(2\pi\hbar)^2 c}\sqrt{2mkT\pi}\frac{1}{\sinh[\mu_B B/kT]}. \qquad (5.36)$$

Substituting the resulting statistical sum into the expression (5.34), we get

$$M = -n\mu_B\Big[\coth\frac{\mu_B B}{kT} - \frac{kT}{\mu_B B}\Big]. \qquad (5.37)$$

From Eq. (5.37) it follows that in the classical limit the magnetic moment actually disappears, because for $\hbar \to 0$ $\mu_B \to 0 \Longrightarrow M \to 0$.

In the case of $\mu_B B/kT \ll 1$

$$\chi_{dia} = \frac{M}{B} = -\frac{n\mu_B^2}{3kT}. \qquad (5.38)$$

When obtaining Eq. (5.38), Boltzmann statistics was used, i.e. The Pauli exclusion principle was not taken into account. It is possible to strictly obtain the correct expression for the diamagnetic susceptibility of a gas of non-interacting electrons taking into account the Pauli principle, i.e. using Fermi-Dirac statistics, but this calculation is computationally quite cumbersome and therefore we will obtain the correct answer from qualitative considerations. The exact calculation can be found, for example, in the book [10]. In fact, all states up to the Fermi

energy in an electron gas are occupied by electrons. Therefore, a magnetic field cannot change the electron distribution functions. Only in a narrow band $\sim kT$ near the Fermi energy are there free states. Therefore, the formula we obtained should be applied only to these electrons. In order of magnitude, the number of such electrons per unit volume is $n' \sim nkT/E_F$. To get an exact answer, we need to take $n' = 3nkT/2E_F$. Substituting this expression for concentration in (5.38), we get

$$\chi_{dia} = -\frac{n\mu_B^2}{2E_F}. \tag{5.39}$$

Taking into account the expression (5.22), this formula can be rewritten as:

$$\chi_{dia} = -\frac{1}{3}\chi_{Pauli}. \tag{5.40}$$

Thus, for a gas of free electrons, Pauli paramagnetism always prevails over Landau diamagnetism and the total response of the gas to a magnetic field is paramagnetic. However, in real materials this may not be the case. The point is that when taking into account the interaction of an electron with a periodic lattice potential, the mass of a free electron must be replaced by the effective mass $m \to m^*$. This leads to the fact that in the expression for diamagnetic susceptibility (5.39) $\mu_B \to \mu^* = e\hbar/2m^*c = (m/m^*)\mu_B$. In the expression (5.22) for the paramagnetic Pauli susceptibility, such a replacement does not need to be made, because this includes the electron's own (spin) momentum, which is not associated with orbital motion. Therefore, the final susceptibility of the electron gas can be written as

$$\chi = \chi_{Pauli} + \chi_{dia} = \frac{n\mu_B^2}{2E_F}\big(3 - \frac{m^2}{m^{*2}}\big). \tag{5.41}$$

This result allows to explain the negative susceptibility of conduction electrons of some metals, such as beryllium and bismuth. In addition, a situation where Landau diamagnetism

prevails over Pauli paramagnetism occurs in doped semiconductors, for which $m^* \ll m$ in the impurity band. Then, the susceptibility of a pure semiconductor without impurities, which is associated with the Landau diamagnetism of the ionic cores, is first measured, and then it is subtracted from the susceptibility of the doped semiconductor. The resulting susceptibility is related to the susceptibility of conduction electrons in the impurity band.

Most metals belong to transition elements; their magnetic properties are associated with d- or f-shells. Metals that have completely filled inner shells are called simple intransition metals. These include elements of groups I and II, Al, Ga, In and Ti from group III, Sn and Pb from group IV, As, Sb and Bi from group V, Te, Po from group VI. Their susceptibility is determined by the diamagnetic susceptibility of ions and the susceptibility of conduction electrons.

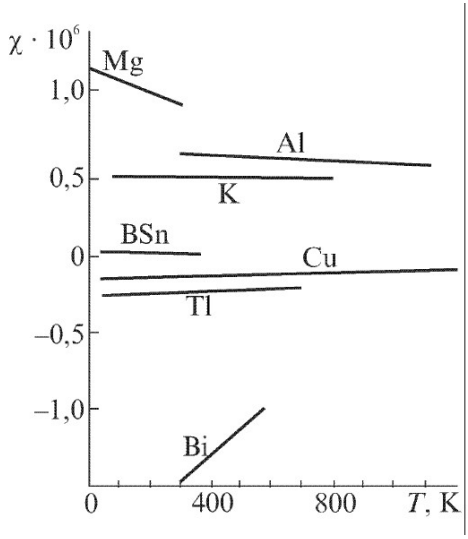

Figure 5.4: Temperature dependence of the susceptibility of some metals. From [7].

The characteristic values and temperature dependence of the susceptibility of some metals are shown in Fig. 5.4. It can be seen that for most non-transition and even some transition metals the temperature dependence of susceptibility is weak, i.e. their behavior is qualitatively described by the free electron model. Quantitative comparison is difficult due to the contribution of the diamagnetic susceptibility of the ions, which can only be determined from indirect data.

Chapter 6

Ferromagnetism and antiferromagnetism.

6.1 Exchange interaction

The main feature of ferromagnets is the presence of spontaneous magnetization without the application of an external magnetic field. The basic properties of ferromagnets are satisfactorily explained if we assume that there is some interaction leading to a gain in energy when the electron spins are oriented in parallel. The energy of such interaction per particle should be $A_1 \sim 0.1$ eV.

The simplest assumption about the nature of this interaction - the interaction of magnetic dipoles - is not suitable for quantitative reasons. Indeed, the energy of such interaction is $\sim \mu_B^2/a_B^3 \sim 10^{-16} erg \sim 10^{-4}$eV.

We know of only two types of forces that play a significant role in atomic phenomena - magnetic and electric. It remains to assume that the interaction between the spins of electrons in a ferromagnet is caused by electric forces. The energy of electrostatic interaction of electrons in an atom is $\sim e^2/a_B \sim$

$10^{-12} erg \sim 1$eV. Even a small part of it is enough to achieve the desired effect.

It seems strange that electrostatic interaction can change magnetic properties. In addition, it is known that in the ground state of a Fermi gas the minimum energy is achieved when electrons occupy all the lower energy levels with opposite spins. But in 1926, Frenkel and Heisenberg independently suggested that, under certain conditions, a minimum electrostatic energy would be achieved for parallel orientation of electron spins. The theory of ferromagnetism they proposed was a generalization of the simplest problem of quantum chemistry - the problem of the properties of the hydrogen molecule. Therefore, this task will be considered in the next paragraph.

6.1.1 Hydrogen molecule.

The hydrogen molecule consists of two protons and two electrons. The designations of all distances between these particles in a hydrogen molecule are shown in Fig. 6.1.

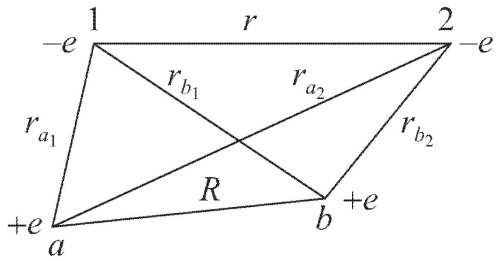

Figure 6.1: Definition of distances in a hydrogen molecule. From [7].

Due to the large mass of the nuclei, they can be considered immobile. The task is to determine the energy of the system depending on the distance R between the nuclei. The

Schrödinger equation for the entire molecule is:

$$\left\{\Delta_1 + \Delta_2 + \frac{2m}{\hbar^2}[E - V(R, r, r_{a_1}, r_{a_2}, r_{b_1}, r_{b_2})]\right\}\psi = 0, \quad (6.1)$$

where $V = e^2/R + e^2/r - e^2/r_{a_1} - e^2/r_{a_2} - e^2/r_{b_1} - e^2/r_{b_2}$, $\psi = \psi(x_1, y_1, z_1, x_2, y_2, z_2)$ depends on the coordinates of both electrons. $\Delta_{1,2} = \partial^2/\partial x_{1,2} + \partial^2/\partial y_{1,2} + \partial^2/\partial z_{1,2}$.

It is impossible to solve Eq. (6.1) exactly, so we will solve it approximately. As a zero approximation, we choose the case of nuclei at infinity $R = \infty$. Then the problem splits into 2 problems about the hydrogen atom. Let E_0 be the energy of the lowest level of the hydrogen atom. Let us assume that the first electron is located near the nucleus a, then the wave function depends only on the coordinates of the first electron $q_1 = (x_1, y_1, z_1)$. The wave function of the lowest level obeys the Schrödinger equation:

$$\left[\Delta_1 + \frac{2m}{\hbar^2}(E_0 - \frac{e^2}{r_{a_1}})]\right]\psi_a(q_1) = 0. \quad (6.2)$$

For the second electron, which is located near the b nucleus, the Schrödinger equation takes the form:

$$\left[\Delta_2 + \frac{2m}{\hbar^2}(E_0 - \frac{e^2}{r_{b_2}})]\right]\psi_b(q_2) = 0. \quad (6.3)$$

If we consider these two individual atoms as a single system, then its total wave function is $\psi(q_1, q_2) = \psi_a(q_1)\psi_b(q_2)$, and its energy is $E = 2E_0$. But a state is also possible when the second electron is near the nucleus a, and the first electron is near the nucleus b. The wave function of such a state is $\psi_b(q_1)\psi_a(q_2)$, and the energy is still $2E_0$. Due to the principle of superposition, an arbitrary state of the system is described by a wave function of the form

$$\psi_0 = \alpha\psi_a(q_1)\psi_b(q_2) + \beta\psi_b(q_1)\psi_a(q_2). \quad (6.4)$$

We will consider the functions $\psi_{a,b}(q)$ to be normalized, i.e.

$$\int dq|\psi_{a,b}(q)|^2 = 1. \tag{6.5}$$

We will also consider them orthogonal, i.e.

$$\int dq\psi_a^*(q)\psi_b(q) = 0. \tag{6.6}$$

The assumption of orthogonality is based on the fact that the wave functions $\psi_{a,b}$ decrease quite rapidly with distance from the nucleus. As the nuclei come closer, they begin to overlap, see Fig. 6.2 and the orthogonality condition is not satisfied exactly, but this correction is small.

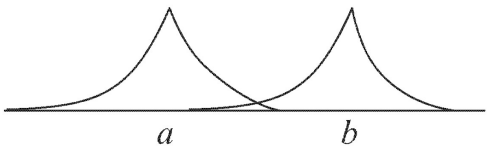

Figure 6.2: Overlap of electron wave functions in the hydrogen molecule. From [7].

Let's move on to consider the first approximation. When the nuclei come closer, the terms of the potential energy of interaction of electrons with each other and with the nuclei not taken into account in (6.2)-(6.3) will lead to a change in the eigenvalues of the energy of the system $E = 2E_0 + E'$. Substituting the wave function (6.4) and the energy $2E_0 + E'$ into the complete Schrödinger equation (6.1) leads to

$$\alpha\Big[E' - \frac{e^2}{R} - \frac{e^2}{r} + \frac{e^2}{r_{b_1}} + \frac{e^2}{r_{a_2}}\Big]\psi_a(q_1)\psi_b(q_2) +$$
$$\beta\Big[E' - \frac{e^2}{R} - \frac{e^2}{r} + \frac{e^2}{r_{a_1}} + \frac{e^2}{r_{b_2}}\Big]\psi_a(q_2)\psi_b(q_1) = 0. \tag{6.7}$$

By multiplying the equation (6.7) by $\psi_a^*(q_1)\psi_b^*(q_2)$ and integrating over $q_{1,2}$, and then multiplying the same equation (6.7) on $\psi_a^*(q_2)\psi_b^*(q_1)$ and again integrating over $q_{1,2}$, we obtain two algebraic equations:

$$\alpha(E' - C) - \beta A = 0, \tag{6.8}$$
$$\alpha A - \beta(E' - C) = 0, \tag{6.9}$$

where

$$C = \frac{e^2}{R} + \int \Big(\frac{e^2}{r} - \frac{e^2}{r_{b_1}} - \frac{e^2}{r_{a_2}}\Big)|\psi_a(q_1)|^2|\psi_b(q_2)|^2 dq_1 dq_2 \tag{6.10}$$

is the conventional electrostatic energy of interaction, because $e|\psi(q)|^2$ expresses the electric charge density at a given point.

$$A = \int \Big(\frac{e^2}{r} - \frac{e^2}{r_{a_1}} - \frac{e^2}{r_{b_2}}\Big)\psi_a^*(q_1)\psi_b(q_1)\psi_b^*(q_2)\psi_a(q_2) dq_1 dq_2 \tag{6.11}$$

cannot be interpreted in a similar simple way. Obviously, this is also some kind of energy of electrostatic interaction, which has no classical analogue. Its appearance is associated with the indistinguishability of electrons in quantum mechanics. The quantity A is called the exchange energy or exchange integral.

A nontrivial solution of the system (6.9) with respect to α and β is possible if its determinant is zero.

$$det \begin{pmatrix} E' - C & -A \\ A & -(E' - C) \end{pmatrix} = 0 \Rightarrow \tag{6.12}$$
$$E' = C \pm A, \quad \alpha = \pm\beta. \tag{6.13}$$

Consequently, the solution to the Schrödinger equation (6.1) in this approximation takes the form

$$\psi_0^{(1)} = \alpha\big[\psi_a(q_1)\psi_b(q_2) + \psi_a(q_2)\psi_b(q_1)\big], E^{(1)} = 2E_0 + C + A \tag{6.14}$$
$$\psi_0^{(2)} = \alpha\big[\psi_a(q_1)\psi_b(q_2) - \psi_a(q_2)\psi_b(q_1)\big], E^{(2)} = 2E_0 + C - A. \tag{6.15}$$

The degenerate ground state of the zeroth approximation splits into two. Depending on the sign of the exchange integral, any of them can be energetically more favorable.

In our derivation, we did not take into account the electron's spin and magnetic moment, but only the electrostatic interaction. However, it turns out that each of the wave functions (6.15) is associated with a certain value of the total electron spin. The full wave function must depend not only on the coordinates, but also on the spins of the electrons. Let $\sigma_{1,2}$ be the spin quantum numbers of electrons, showing the projection of their spins onto the quantization axis. Then the total wave system of two electrons is

$$\psi(q_1, q_2, \sigma_1, \sigma_2) = \psi_0(q_1, q_2)\varphi(\sigma_1, \sigma_2). \tag{6.16}$$

The total electron wave function must be antisymmetric with respect to the pairwise permutation of any electrons, i.e. in our case, two electrons change sign with a simultaneous rearrangement of the spatial and spin coordinates of the electrons. This requirement is a consequence of the principle of particle indistinguishability in quantum mechanics. The Pauli principle follows from it as a special case, because the antisymmetric function vanishes when the coordinates coincide. The requirement that the total wave function be antisymmetrical leads to the fact that, with a symmetric coordinate wave function, the spin function must be antisymmetric and vice versa.

If the total spin of two electrons is equal to unity, then the spin wave function will be symmetric. If zero, then antisymmetric. Therefore, the state $\psi_0^{(1)}$, which has a symmetric coordinate wave function, corresponds to zero total electron spin, and the solution $\psi_0^{(2)}$, whose wave function is antisymmetric, corresponds to a total spin equal to one. Thus, the energy of a hydrogen molecule turns out to be related to the mutual arrangement of electron spins in the molecule. Depending on the sign of the exchange integral, either the total

spin zero or the total spin one may be more advantageous. It should be emphasized once again that the indicated difference in energies is associated not with the magnetic interaction of electrons, but with the electrostatic one.

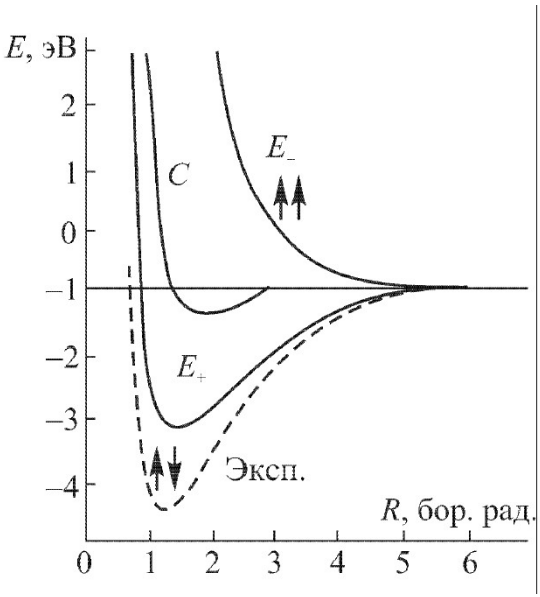

Figure 6.3: The energy of interaction between two hydrogen atoms. From [7].

Figure 6.3 shows the dependence of the energy of a hydrogen molecule on the distance between nuclei, expressed in Bohr radii. For a hydrogen molecule at distances greater than the Bohr radius $A < 0$, therefore the more favorable state is $E^{(1)}$, corresponding to zero total spin of the electrons. The minimum of this energy determines the equilibrium distance between nuclei and the dissociation energy of the molecule. For comparison, the dotted line shows the experimental dependence of the ground state energy on the distance between nuclei. There is good agreement with our simplified calculation. At very small distances between nuclei, the exchange

integral changes sign and a state with a total electron spin of 1 becomes more favorable. But in practice, too high pressures are required to achieve this state.

Now we will consider the hydrogen molecule as a two-level system, i.e. let us assume that the molecule can only be in the states $E^{(1)} \equiv E_s$ and $E^{(2)} \equiv E_t$, all other excited states of the molecule are too high in energy and it practically cannot go there. Let us write the Hamiltonian of such a two-level system, acting only on the spin degrees of freedom of the electrons. It is obvious that the eigenstates of such a Hamiltonian will be states with total spin $S_{tot} = 0$ and total spin $S_{tot} = 1$ and when acting on a state with $S_{tot} = 0$ the Hamiltonian must produce an eigenvalue E_s, and when acting on a state with $S_{tot} = 1$ - E_t. We will look for the Hamiltonian in the form:

$$\hat{H}_{spin} = M_1 + M_2 \hat{\boldsymbol{s}}_1 \hat{\boldsymbol{s}}_2, \tag{6.17}$$

where $M_{1,2}$ are the constants that need to be found, and $\hat{\boldsymbol{s}}_{1,2}$ are the spin operators of the first and second electrons.

The scalar product $\hat{\boldsymbol{s}}_1 \hat{\boldsymbol{s}}_2$ has a certain value in a state with a certain total spin of two electrons. Let's find it.

$$\hat{\boldsymbol{s}}_1 \hat{\boldsymbol{s}}_2 = \frac{1}{2}\big[(\hat{\boldsymbol{s}}_1 + \hat{\boldsymbol{s}}_2)^2 - \hat{\boldsymbol{s}}_1^2 - \hat{\boldsymbol{s}}_2^2\big]. \tag{6.18}$$

Taking the average value of this operator over a state with a certain value S_{tot}, we obtain:

$$\langle \hat{\boldsymbol{s}}_1 \hat{\boldsymbol{s}}_2 \rangle = \frac{1}{2}\big[S_{tot}(S_{tot}+1) - 2s(s+1)\big], \tag{6.19}$$

where $s = 1/2$ is the spin of one electron. From (6.19) we get:

$$\begin{aligned} \langle \hat{\boldsymbol{s}}_1 \hat{\boldsymbol{s}}_2 \rangle &= -\frac{3}{4}, \quad S_{tot} = 0 \\ \langle \hat{\boldsymbol{s}}_1 \hat{\boldsymbol{s}}_2 \rangle &= \frac{1}{4}, \quad S_{tot} = 1. \end{aligned} \tag{6.20}$$

Taking into account Eqs. (6.20), we can find the constants M_1 and M_2 from the conditions $\langle S_{tot}=0|\hat{H}|S_{tot}=0\rangle = E_s$ and $\langle S_{tot}=1|\hat{H}|S_{tot}=1\rangle = E_t$:

$$\hat{H}_{spin} = \frac{1}{4}(E_s + 3E_t) - (E_s - E_t)\hat{\boldsymbol{s}}_1\hat{\boldsymbol{s}}_2. \tag{6.21}$$

6.1.2 Heisenberg Hamiltonian.

Heisenberg's original calculations were a direct generalization of the problem of the hydrogen molecule. A system consisting of N hydrogen-like atoms whose electrons are in the S-state was considered. The Hamiltonian of such a system has the form:

$$\hat{H} = -\frac{\hbar^2}{2m}\sum_{\alpha=1}^{N}\nabla_\alpha^2 + \sum_{\alpha,i} g_i(q_\alpha) + \sum_{\alpha<\alpha'} V_{\alpha\alpha'}(|q_\alpha - q'_\alpha|), \tag{6.22}$$

where $g_i(q_\alpha)$ is the energy of interaction of the αth electron with the nucleus i, and $V_{\alpha\alpha'}(|q_\alpha - q'_\alpha|)$ is the energy interactions of α and α' electrons with each other.

As in the case of the hydrogen molecule, the solution is carried out by the method of successive approximations. In the zero approximation, a system of isolated atoms is considered. The Schrödinger equation for each of them has the form:

$$\Big[-\frac{\hbar^2}{2m}\nabla_\alpha^2 + g_i(q_\alpha)\Big]\varphi_i(q_\alpha) = E_0\varphi_i(q_\alpha). \tag{6.23}$$

The general solution of Eq. (6.23) is represented as a linear combination of products of functions $\varphi_i(q_\alpha)$. Its substitution in (6.22) allows us to find the next approximation for the energy of electronic states taking into account their interaction. The total energy of the system will differ from the energy of the zero approximation by the electrostatic energy of electron

interaction and exchange energy. The exchange integral for two atoms i and j will have the form:

$$A_{ij} = \int \varphi_i^*(q)\varphi_j^*(q')\varphi_i(q')\varphi_j(q) \times \Big[V_{ij}(|q-q'|) + g_i(q') + g_j(q)\Big] dqdq'. \tag{6.24}$$

The contribution to the Hamiltonian from the total energy of the exchange interaction has the form:

$$\hat{H}_{ex} = -2\sum_{ij} A_{ij}\hat{\boldsymbol{s}}_i\hat{\boldsymbol{s}}_j. \tag{6.25}$$

The expression (6.25) is called the Heisenberg Hamiltonian. The original Heisenbang-Frenkel theory of calculating exchange integrals is too oversimplified to be required to be in quantitative agreement with experiment. However, two important fundamental conclusions follow from it: 1) if the exchange integrals are positive, then a state with spontaneous magnetization - ferromagnetism - can arise. 2) The energy of exchange interaction is sufficient for the existence of ferromagnets with a Curie temperature of $\sim 1000K$.

Let us consider under what conditions the exchange integral will be positive. The interaction energy of charges of the same sign is $V_{ij}(|q-q'|) > 0$, and the interaction energy of the opposite charges $g_i(q)$ is negative. Therefore, the following condition must be met:

$$\Big|\int \varphi_i^*(q)\varphi_j^*(q')\varphi_i(q')\varphi_j(q)V_{ij}(|q-q'|)dqdq'\Big| > \Big|\int \varphi_i^*(q)\varphi_j^*(q')\varphi_i(q')\varphi_j(q)[g_i(q') + g_j(q)]dqdq'\Big|. \tag{6.26}$$

The fulfillment of this condition depends on the form of the wave functions of an individual electron $\varphi_i(q)$. If the wave functions φ_i and φ_j are large near the nuclei, then the right-hand side of the expression (6.26) is also large, because g_i

has large values near the core. In this case, the condition for the exchange integral to be positive is not satisfied. That is, for it to be positive, the wave functions near the nuclei must have a smaller value. This condition is satisfied by the wave functions of quantum states with large orbital numbers l. Of course, a shell with a large l value can contain several electrons, but it does not have to be completely filled so that its spin momentum is not zero. These requirements are met by atoms of transition elements.

Further, the wave functions $\varphi_i(q)$ fall off quite rapidly with distance, so the value of those entering into (6.26) is mainly determined by the value of the integrand at the maximum point of the product $\varphi_i^*(q)\varphi_j^*(q')\varphi_i(q')\varphi_j(q)$. In order for the exchange integral to be positive, this maximum must be located away from the nuclei, i.e. The atoms of the ferromagnetic substance must be located sufficiently far from each other.

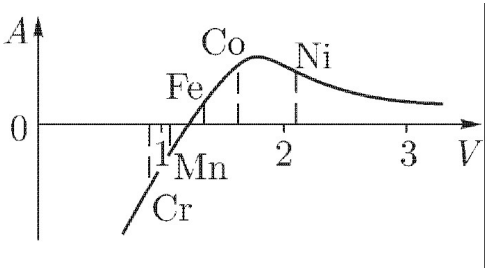

Figure 6.4: The $A(V)$ dependence calculated by Bethe for the d-state. From [7].

In practice, all ferromagnetic elements belong to the transition category. Ferromagnetic alloys and compounds contain transition elements. But only a few transition elements are ferromagnetic. This is explained by the fact that only for a small number of elements the distance between atoms is sufficiently large. More precisely, one should consider the ratio of this distance to the diameter of the inner orbits. Let's de-

note it V. All ferromagnetic elements have $V > 1.5$. Fig. 6.4 shows the dependence $A(V)$ calculated by Bete. It can be seen that for good ferromagnets Fe, Co, Ni, these calculations give a positive value of the exchange integral. For gadolinium and some other rare earth elements, V is already too high, so the exchange integral in them, although positive, is small and the Curie points are low.

Manganese has too small interatomic distance, but is on the verge of changing the sign of the exchange integral, so a small increase in the lattice constant of manganese should turn it into a ferromagnet. Indeed, the addition of small nitrogen impurities to manganese leads to the appearance of ferromagnetism. Some alloys of transition elements and intermetallic compounds are also ferromagnetic. For example, Mn-Cu-Al alloys (Heusler alloys), MnSb, MnBi compounds have ferromagnetic properties.

Because in all cases of the appearance of ferromagnetism it is associated with transition elements, Heisenberg's original consideration of atoms with S electrons is a very rough approximation. However, in most transition metals, magnetism is due only to spin degrees of freedom due to the crystalline Stark effect, which leads to the splitting of electronic states along the projection of the orbital momentum. As a result, the orbital momentum is frozen, i.e. the orbital moments of individual ions do not have the opportunity to reorient. In addition, it must be taken into account that many ferromagnets are metals, which leads to the need to consider the magnetism of conduction electrons and the interaction of s- and d-electrons.

6.2 Weiss model. Ferromagnets.

Ferromagnetism is characterized by the presence of spontaneous magnetization even without the application of an external field. The part of the Hamiltonian of a ferromagnet that describes magnetism, taking into account the external field, has the form:

$$\hat{H} = -\sum_{ij} J_{ij}\hat{\boldsymbol{S}}_i\hat{\boldsymbol{S}}_j + g_J\mu_B\sum_i \hat{\boldsymbol{S}}_i\boldsymbol{B}, \tag{6.27}$$

where $\hat{\boldsymbol{S}}_i$ is the spin operator localized at a given site. Absolute value of spin is S. The exchange integral is $J_{ij} > 0$ and is nonzero only for the nearest neighbors. Let's start with the approximation known as the Weiss model: the interaction of a magnetic ion with its neighbors is described as the appearance of some effective field $\boldsymbol{B}_{mf}$ acting on it:

$$\hat{H} = g_J\mu_B\sum_i \hat{\boldsymbol{S}}_i(\boldsymbol{B} + \boldsymbol{B}_{mf}), \quad \boldsymbol{B}_{mf} = \lambda\boldsymbol{M}. \tag{6.28}$$

Let us find the relation between $\boldsymbol{B}_{mf}$ and the exchange integral $J_{ij} = J_{ex}$:

$$-\sum_{ij} J_{ij}\hat{\boldsymbol{S}}_i\hat{\boldsymbol{S}}_j = -\sum_i (J_{ex}\sum_j \hat{\boldsymbol{S}}_j)\hat{\boldsymbol{S}}_i. \tag{6.29}$$

Next, the operator sum in parentheses in (6.29) is replaced by its average value, i.e. classic expression. Then the exchange contribution to the Hamiltonian for the ith electron can be written as:

$$\hat{H}_{i,mf} = -g_J\mu_B\hat{\boldsymbol{S}}_i\frac{J_{ex}\sum\limits_j g_J\mu_B\boldsymbol{S}_j}{g_J^2\mu_B^2} = g_J\mu_B\hat{\boldsymbol{S}}_i\frac{J_{ex}Z\langle\mu_j\rangle}{g_J^2\mu_B^2} = g_J\mu_B\hat{\boldsymbol{S}}_i\frac{J_{ex}Z\boldsymbol{M}}{ng_J^2\mu_B^2} = g_J\mu_B\hat{\boldsymbol{S}}_i\boldsymbol{B}_{mf}, \tag{6.30}$$

where Z is the number of nearest neighbors of ion i. From (6.30) one can find the value of the effective field

$$\boldsymbol{B}_{mf} = \frac{J_{ex} Z \boldsymbol{M}}{n g_J^2 \mu_B^2} = \lambda \boldsymbol{M}, \quad \lambda = \frac{J_{ex} Z}{n g_J^2 \mu_B^2}. \tag{6.31}$$

In the Weiss model we have a situation similar to a paramagnet in the field $\boldsymbol{B} + \boldsymbol{B}_{mf}$. Therefore, according to Eq. (4.13), the magnetization of a ferromagnet obeys the equation

$$\frac{\boldsymbol{M}}{M_s} = B_J(y), \tag{6.32}$$

where

$$B_J(y) = \frac{2J+1}{2J} \coth\Big[\frac{2J+1}{2J} y\Big] - \frac{1}{2J} \coth\Big[\frac{y}{2J}\Big], \tag{6.33}$$

$$y = \frac{g_J \mu_B J (B + \lambda M)}{kT}. \tag{6.34}$$

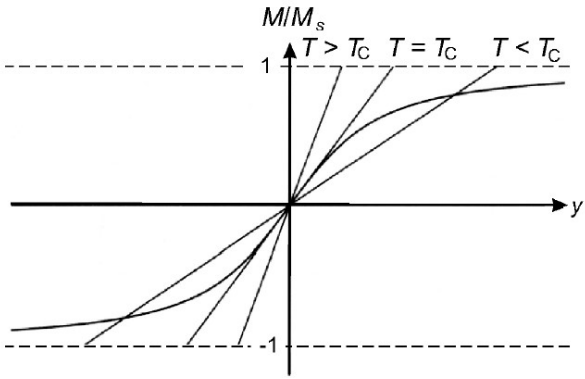

Figure 6.5: Graphical solution of Eq. (6.32) at $\boldsymbol{B} = 0$. From [5].

In the absence of an external field $B = 0$, magnetization obeys Eq. (6.32), in which $y = g_J\mu_B J\lambda M/(kT)$. The graphical solution of this equation is presented in Fig. 6.5. It is represented by the points of intersection of the Brillouin function and the straight line $M/M_s = (kT/g_J\mu_B J\lambda M_s)y$. The solution $M = 0$ always exists. In addition to this, for sufficiently small slopes of the straight line $M/M_s = (kT/g_J\mu_B J\lambda M_s)y$ there are also 2 non-zero solutions for magnetization, which are equal in magnitude, but have opposite signs. The slope of the straight line is determined by temperature, so a non-zero solution, i.e. spontaneous magnetization exists below a certain critical temperature T_c - the Curie temperature. Let's find it. It is obvious that the Curie temperature is determined by the slope of the straight line, which coincides with the slope of the Brillouin function at $y = 0$. Therefore, to find it, we need to solve the equation

$$\frac{d(M/M_s)}{dy} = \frac{dB_J(y)}{dy}\Big|_{y=0}. \tag{6.35}$$

Because $B_J(y) \approx [(J+1)/3J]y$ for $y \to 0$, then from (6.35) we obtain

$$T_c = \frac{(J+1)g_J\mu_B\lambda M_s}{3k}. \tag{6.36}$$

Using expressions for saturation magnetization $M_s = ng_J\mu_B J$ and effective magnetic moment $\mu_{eff} = g_J\mu_B\sqrt{J(J+1)}$, the formula for the critical temperature can be rewritten as

$$T_c = \frac{n\lambda\mu_{eff}^2}{3k}. \tag{6.37}$$

The molecular (effective) Weiss field can be estimated through the critical temperature:

$$B_{mf} = \lambda M_s = \frac{3kT_c}{g_J\mu_B(J+1)}. \tag{6.38}$$

Using typical values of $J = 1/2$, $T_c = 10^3 K$, we obtain $B_{mf} =$ 1500T. This is a very high magnetic field, clearly indicating the strength of the exchange interaction between spins.

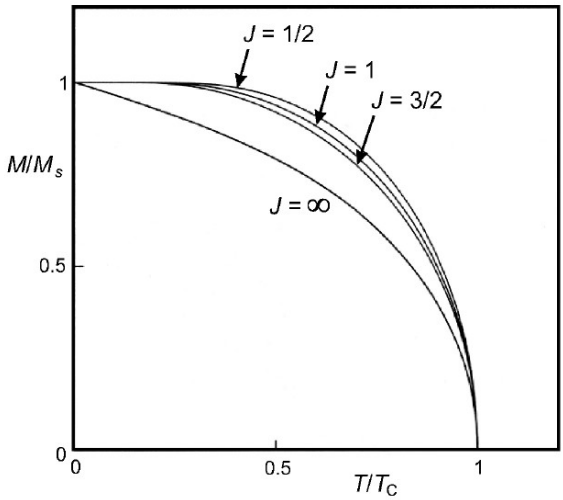

Figure 6.6: Magnetization of a ferromagnet in the Weiss model as a function of temperature for different values of the total angular momentum of the magnetic ion J. From [5].

The result of the numerical solution of Eq. (6.32) in the absence of an external field is shown in Fig. 6.6. Analytically, one can find the behavior of magnetization near the critical temperature and near zero temperature. Let's do it. First consider $M(T)$ for $T \to T_c$. Moreover, $M \to 0 \Longrightarrow y \to 0$. The expansion of the Brillouin function for small values of y has the form:

$$B_J(y) = \frac{J+1}{3J} y - \frac{(J+1)(2J^2+2J+1)}{90J^3} y^3. \qquad (6.39)$$

Substituting $y = (3J/J+1)(M/M_s)(T_c/T)$ into (6.39), from (6.32) we obtain the following equation for finding magnetiza-

tion:

$$\frac{M}{M_s} = \frac{M}{M_s}\frac{T_c}{T}\Big(1 - \Big(\frac{M}{M_s}\Big)^2\Big(\frac{T_c}{T}\Big)^2\frac{3(2J^2+2J+1)}{10(J+1)^2}\Big), \quad (6.40)$$

from which we obtain the answer for magnetization near the critical temperature:

$$\Big(\frac{M}{M_s}\Big)^2 = \frac{10(J+1)^2}{3(J^2+(J+1)^2)}\Big(1-\frac{T}{T_c}\Big)\Big(\frac{T}{T_c}\Big)^2. \quad (6.41)$$

Thus, we find that at $T \to T_c$ the magnetization behaves as $M/M_s \propto \sqrt{1-T/T_c}$.

Now let's find the behavior of magnetization at $T \to 0$. $y = (3J/J+1)(M/M_s)(T_c/T) \to \infty$ for $T \to 0$. Using the asymptotic behavior of the cotangent $\coth x \approx 1 + 2e^{-2x}$ for $x \to \infty$, we obtain:

$$\frac{M}{M_s} \approx 1 - \frac{1}{J}e^{-\frac{3T_cM}{(J+1)TM_s}} = 1 - \frac{1}{J}e^{-c/T}. \quad (6.42)$$

Thus, at low temperatures in the Weiss model, the deviation of magnetization from its value at zero temperature is exponentially small.

Let us find in the Weiss approximation the susceptibility of the ferromagnet at $T > T_c$. Let a weak external field $\boldsymbol{B}$ be applied. Then the argument of the Brillouin function y is small and we can use the expansion $B_J(y) \approx [(J+1)/3J]y$. Then we get:

$$\frac{M}{M_s} = \frac{g_J\mu_B(J+1)}{3k}\frac{B+\lambda M}{T} = \frac{T_c}{\lambda M_s}\frac{B+\lambda M}{T} \Longrightarrow$$
$$\frac{M}{M_s} = \frac{T_cB}{\lambda M_s}\frac{1}{T-T_c}. \quad (6.43)$$

Where do we get the Curie-Weiss law for susceptibility:

$$\chi = \frac{T_c}{\lambda}\frac{1}{T-T_c} = \frac{c}{T-T_c}. \quad (6.44)$$

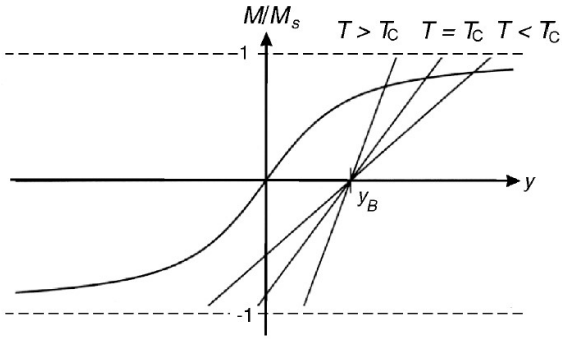

Figure 6.7: Graphical method for determining magnetization in the presence of an external field. From [5].

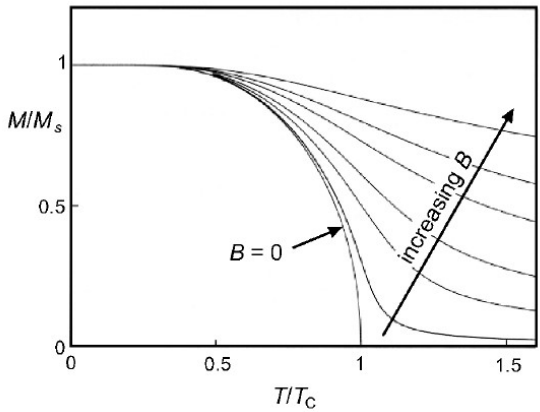

Figure 6.8: Magnetization of a ferromagnet in the Weiss model as a function of temperature for $J = 1/2$ and different values of the external field. From [5].

If we now give up the condition of a small external magnetic field, then Eq. (6.32) for magnetization can again be solved graphically. The difference with the case $B = 0$ is that now we are looking for intersections of the Brillouin function with the line $M/M_s = (kT/g_J\mu_B J\lambda M_s)y - B/(\lambda M_s)$, not pass-

ing through the origin, see Fig. 6.7. It is obvious that in this case a non-zero solution for magnetization exists at any temperature. Thus, in an external field the phase transition at $T = T_c$ disappears.

6.3 Magnetism of itinerant electrons. Stoner instability

The Heisenberg Hamiltonian discussed above describes a system of localized spins. However, it is obvious that there must be an exchange interaction of the same nature between itinerant electrons in metals. To accurately calculate the electronic spectra and magnetic properties of a metal taking into account this exchange interaction, it is necessary to know the exact many-particle wave function of itinerant electrons, which is a very difficult task. However, the basic magnetic properties of a system of itinerant electrons can be understood within the framework of a molecular field model similar to that discussed above for a system of localized spins. Let us assume that each electron of a free Fermi gas is acted upon by an effective field proportional to the magnetization of this gas $\boldsymbol{H}_{eff} = \lambda \boldsymbol{M}$ and study the problem of the possibility of the occurrence of *spontaneous* magnetization in such a system.

In order for a magnetic moment to arise in the system, it is necessary for some of the electrons to flip their spin and, accordingly, move from the $\downarrow$ spin subband to the $\uparrow$ spin subband, see Fig. 6.9. This is accompanied by a loss in the kinetic energy of the system. Indeed, each of the transferring electrons with energy $E_F - \delta\varepsilon$ increases its energy by $2\delta\varepsilon$. If electrons transfer in the δE band, then the total change in the kinetic

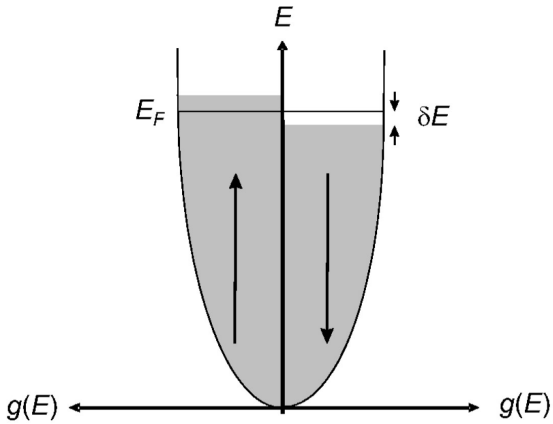

Figure 6.9: Toward the calculation of spontaneous splitting of the density of states of electrons in a Fermi gas without the application of an external magnetic field. From [5].

energy of electrons

$$\Delta E_{kin} = 2\int_0^{\delta E} d(\delta\varepsilon)\frac{g(E_F)}{2}\delta\varepsilon = \frac{g(E_F)}{2}\delta E^2, \tag{6.45}$$

where $g(E_F)$ is the total density of states at the Fermi level per 2 spins. This redistribution of electrons leads to a difference in electron concentrations for spins up and down:

$$n_{\uparrow,\downarrow} = \frac{1}{2}n \pm \frac{1}{2}g(E_F)\delta E, \tag{6.46}$$

which, in turn, generates non-zero magnetization in the system:

$$M = \mu_B(n_\uparrow - n_\downarrow) = \mu_B g(E_F)\delta E. \tag{6.47}$$

In the molecular field model, magnetization generates an effective field in which the magnetic moment of the gas acquires potential energy

$$\Delta E_{pot} = -\frac{1}{2}\boldsymbol{M}(\lambda\boldsymbol{M}) = -\frac{1}{2}Ug^2(E_F)\delta E^2, \tag{6.48}$$

where the notation $U = \lambda\mu_B^2$ is introduced. The total change in the energy of the Fermi gas as a result of the occurrence of spontaneous magnetization:

$$\Delta E = \Delta E_{kin} + \Delta E_{pot} = \frac{1}{2} g(E_F)(1 - Ug(E_F))\delta E^2. \quad (6.49)$$

Magnetization occurs spontaneously if $\Delta E < 0 \Longrightarrow$

$$Ug(E_F) \geq 1. \quad (6.50)$$

This condition represents a criterion for the instability of a conduction electron gas with respect to the occurrence of ferromagnetism (Stoner instability criterion). It is worth noting that, in contrast to the Weiss model for localized spins, where spontaneous magnetization appears at any arbitrarily small value of λ, even at low temperatures, here at small values of λ ferromagnetism does not appear, because the energy gain due to potential energy is compensated by the loss in kinetic energy, which is absent in the localized spin model.

In the case of $Ug(E_F) < 1$, spontaneous magnetization does not occur, but, nevertheless, the magnetic susceptibility differs from its paramagnetic value. Indeed, let an external magnetic field B be applied to the system. Then the total change in the energy of the system due to the occurrence of magnetization:

$$\Delta E = \frac{1}{2} g(E_F)(1 - Ug(E_F))\delta E^2 - \boldsymbol{MB} = \frac{M^2}{2\mu_B^2 g(E_F)}(1 - Ug(E_F)) - MB. \quad (6.51)$$

From the condition $\partial E/\partial M = 0$ it follows

$$M = \frac{\mu_B^2 g(E_F) B}{1 - Ug(E_F)}, \quad (6.52)$$

that is

$$\chi = \frac{\mu_B^2 g(E_F)}{1 - U g(E_F)} = \frac{\chi_{Pauli}}{1 - U g(E_F)}. \tag{6.53}$$

That is $\chi > \chi_{Pauli}$ due to the Coulomb interaction. This is called Stoner's susceptibility enhancement.

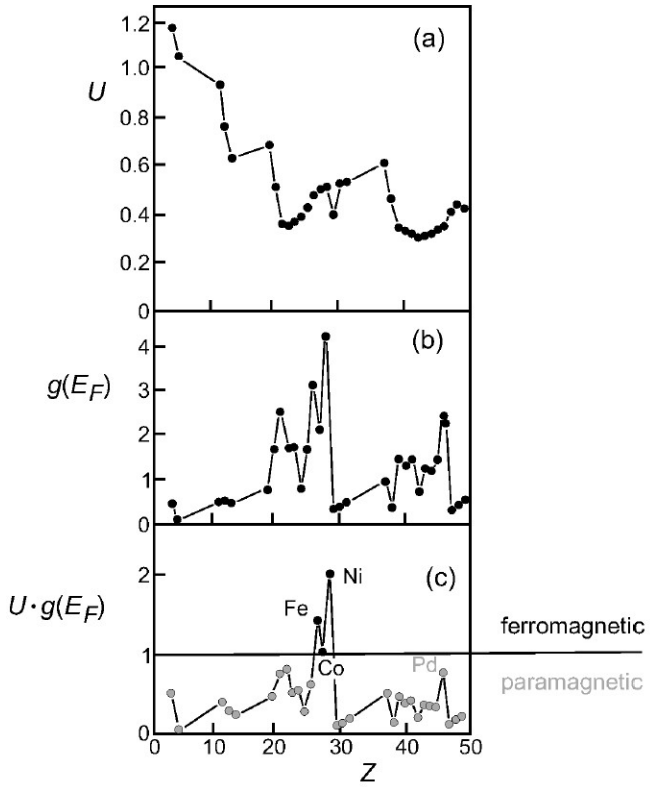

Figure 6.10: Values of the Stoner parameter U, density of states at the Fermi level and their product for the first 50 elements in arbitrary units. From [5].

The values of the Stoner parameter U, the density of states at the Fermi level and their product are shown in Fig. 6.10 for

the first 50 elements. It can be seen that only Fe, Co and Ni, which are indeed ferromagnetic metals, directly satisfy the Stoner criterion. An example of an "almost" ferromagnetic metal is Pd, which is close to the Stoner instability threshold and therefore has a large paramagnetic susceptibility value. Even a small amount of Fe is enough to make PdFe alloy ferromagnetic.

From the data presented it is clear that the fulfillment of the Stoner criterion is ensured, first of all, by the large value of the density of states at the Fermi level in a given metal. In transition metals, two groups of electrons can be conventionally distinguished, which are called s-electrons or conduction electrons and d-electrons or localized electrons responsible for magnetism. Due to the strong overlap of the electron shells of individual atoms, both groups of electrons are collectivized and their energy spectrum forms bands. Each group of electrons can be described by the Bloch wave function

$$\begin{aligned} \psi_s(\boldsymbol{k}, \boldsymbol{r}) &= e^{i\boldsymbol{k}\boldsymbol{r}} u_s(\boldsymbol{k}, \boldsymbol{r}), \\ \psi_d(\boldsymbol{k}, \boldsymbol{r}) &= e^{i\boldsymbol{k}\boldsymbol{r}} u_d(\boldsymbol{k}, \boldsymbol{r}). \end{aligned} \tag{6.54}$$

Periodic functions $u_s(\boldsymbol{k}, \boldsymbol{r})$ are delocalized, and $u_d(\boldsymbol{k}, \boldsymbol{r})$ are highly localized and have pronounced probability density maxima at the locations of ions. Accordingly, the energy bands corresponding to s-electrons are wide and the density of states in them is low, and the d-bands are narrow and the density of states in them is of great importance. Further, in the simplest approximation in the so-called "hard band" model, different elements, having different numbers of itinerant electrons per atom, differ only in the location of the Fermi level. In transition elements, the Fermi level usually falls in the d-band, see Fig. 6.11. If it falls in the middle of the d-band, then the density of states at the Fermi level is maximum and the Stoner criterion is satisfied. In non-transition elements, the Fermi level does not fall into the d-band, the density of states at the

Fermi level is small and the Stoner criterion is not satisfied.

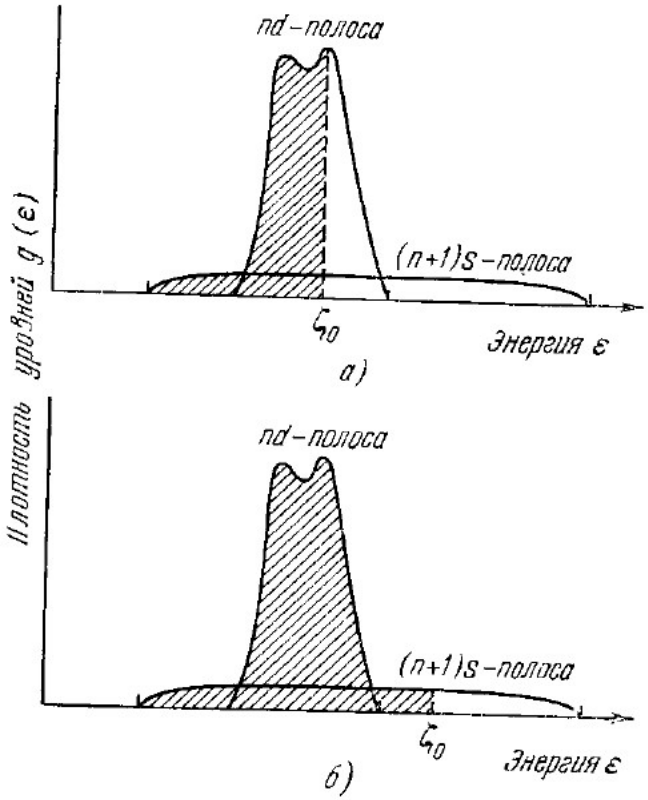

Figure 6.11: Density of states of electrons in overlapping s- and d-bands. (a)-transition metal, the Fermi level lies in the d-band; (b)-non-transition metal, the Fermi level lies in the s-band outside the d-band. The areas filled with electrons at $T = 0$ are shaded. From [11].

When spontaneous magnetization occurs in equilibrium, the filling levels in both spin subbands should be shifted with respect to each other, but as a result of the appearance of the electron potential energy in the effective field, the bottom of the spin subbands shifts by $\pm\delta E$, see Fig. 6.12. If the Stoner

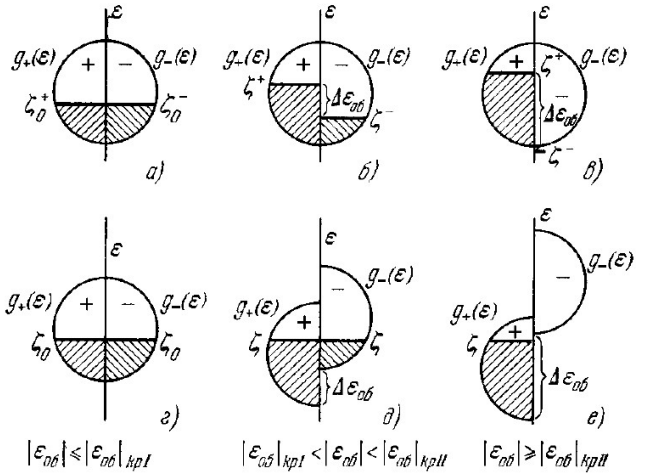

Figure 6.12: Shifting of the spin subbands of itinerant electrons in a metal under the influence of exchange interaction. From [11].

instability does not occur, the bottom of the bands does not shift despite the presence of a nonzero exchange interaction, Fig. 6.12(a) and (d). If Stoner instability occurs, but the value of δE is less than a certain critical value, Fig. 6.12(b) and (e), the density of electronic states in the conduction band is nonzero for both spin subbands. If the magnitude of the exchange interaction is so great that the separation of the bands is large and the density of states at the Fermi level is nonzero only in one of the spin subbands, as in Fig. 6.12(c) and (f), then this is the case of a halfmetal, when all conducting carriers have the same spin.

Often d-electrons in transition metals are considered to be completely localized. Localized electrons are thought to be responsible for magnetism, and collective s-electrons are thought to be responsible for conductivity. Then, in the Hamiltonian of the system, the interaction of d-electrons with each other

is taken into account within the framework of the Heisenberg model, but in addition, their exchange interaction with s-conduction electrons is taken into account. This approach is called the s-d model and is widely used, in particular, in spintronics to describe the effects of controlling the magnetization of a magnet by electric currents.

6.4 Weiss model. Antiferromagnets.

For an antiferromagnet, the exchange integral between the nearest neighbors has a negative sign. Antiferromagnetism can be described by dividing the ion lattice into 2 sublattices. Inside each of the sublattices, the magnetic ordering is ferromagnetic. The orientation of the magnetic moments between the sublattices is antiparallel. This situation is schematically illustrated in Fig. 6.13.

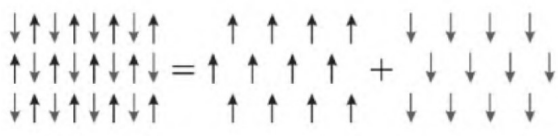

Figure 6.13: The representation of the antiferromagnetic lattice as the sum of two sublattices, inside each of which there is a ferromagnetic ordering. From [5].

Let's start with a simplified consideration of the case when an external magnetic field is not applied and the effective Weiss field acting on each of the sublattices is proportional to the magnetization of the second sublattice:

$$\begin{aligned} \boldsymbol{B}_{mf}^{(1)} &= -|\lambda|\boldsymbol{M}_2, \\ \boldsymbol{B}_{mf}^{(2)} &= -|\lambda|\boldsymbol{M}_1. \end{aligned} \tag{6.55}$$

In this case, the magnetization of each of the sublattices obeys the equation:

$$M_{1,2} = M_s B_J(-\frac{g_J \mu_B J|\lambda| M_{2,1}}{kT}). \tag{6.56}$$

For antiferromagnet $|\boldsymbol{M}_1| = |\boldsymbol{M}_2| = M$. With this in mind, it follows from (6.56)

$$M = M_s B_J(\frac{g_J \mu_B J|\lambda| M}{kT}). \tag{6.57}$$

Thus, in this approximation, the magnetization of each lattice behaves exactly the same as for a ferromagnet and disappears at the Neel temperature T_N, which is determined by the formulas (6.36)-(6.37).

The magnetic susceptibility at temperature $T > T_N$ can be found from the equation:

$$\frac{M}{M_s} = \frac{J+1}{3J} \frac{g_J \mu_B J(B - |\lambda| M)}{kT} = \frac{T_N}{|\lambda| M_s} \frac{B - |\lambda| M}{T}, \tag{6.58}$$

from which we get

$$\frac{M}{M_s} = \frac{T_N B}{|\lambda| M_s} \frac{1}{T + T_N}. \tag{6.59}$$

Magnetic susceptibility obeys the Curie-Weiss law for antiferromagnets:

$$\chi \propto \frac{1}{T + T_N}. \tag{6.60}$$

In the following approximation, it is also necessary to take into account the effective Weiss field from its own sublattice

$$\begin{aligned} \boldsymbol{B}_{mf}^{(1)} &= v_1 \boldsymbol{M}_1 + v_2 \boldsymbol{M}_2, \\ \boldsymbol{B}_{mf}^{(2)} &= v_2 \boldsymbol{M}_1 + v_1 \boldsymbol{M}_2, \end{aligned} \tag{6.61}$$

where $v_2 < 0$. At $B = 0$ we have $\boldsymbol{M}_1 = -\boldsymbol{M}_2 \Longrightarrow$

$$\frac{M_1}{M_s} = B_J\Big(\frac{g_J\mu_B J(v_1 - v_2)M_1}{kT}\Big), \tag{6.62}$$

and we can find the temperature of the Neel in this approximation:

$$T_N = \frac{g_J\mu_B(J+1)(v_1 - v_2)M_s}{3k} = \frac{n(v_1 - v_2)\mu_{eff}^2}{3k} = c(v_1 - v_2). \tag{6.63}$$

Let's apply a small external magnetic field at $T > T_N$ and find the magnetic susceptibility in this approximation:

$$B_J \approx \frac{J+1}{3J}\frac{g_J\mu_B J}{kT}[v_1M_1 + v_2M_2 + B]. \tag{6.64}$$

$$\begin{aligned} M_1 &= \frac{c}{T}(v_1M_1 + v_2M_2 + B), \\ M_2 &= \frac{c}{T}(v_2M_1 + v_1M_2 + B), \end{aligned} \tag{6.65}$$

where $c = (g_J\mu_B(J+1)M_s)/(3k)$. Due to the fact that $B \neq 0$, the condition $\boldsymbol{M}_1 + \boldsymbol{M}_2 = 0$ is no longer fulfilled. Adding up the equations (6.65), for the total magnetization $\boldsymbol{M} = \boldsymbol{M}_1 + \boldsymbol{M}_2$ we get:

$$\boldsymbol{M} = \frac{c}{T}(2\boldsymbol{B} + (v_1 + v_2)\boldsymbol{M}), \tag{6.66}$$

which leads to

$$\boldsymbol{M} = \frac{2c\boldsymbol{B}}{T - c(v_1 + v_2)}. \tag{6.67}$$

For the magnetic susceptibility we obtain:

$$\chi = \frac{2c}{T - \Theta}, \quad \Theta = c(v_1 + v_2). \tag{6.68}$$

Thus, there are 2 characteristic temperatures for an antiferromagnet: T_N is the temperature of disappearance of sublattice magnetization and Θ is the characteristic temperature entering into susceptibility. Their ratio is

$$\frac{T_N}{\Theta} = \frac{v_1 - v_2}{v_1 + v_2}. \tag{6.69}$$

These temperatures merge into one $T_N = -\Theta$ only if we neglect the effective field of our own sublattice, i.e. put $v_1 = 0$.

Now let's consider the behavior of an antiferromagnet at $B \neq 0$ in a weak field at $T < T_N$. We consider the limit of zero temperature, when thermal fluctuations of magnetization relative to the average value can be ignored. The ground state of the system can be found from the minimum energy condition. Given that $\langle \boldsymbol{S}_i^{(\nu)} \rangle = -\boldsymbol{M}_\nu/(g_J \mu_B n)$, where ν is the index of the sublattice, and i is the site number in this sublattice, the expression for the energy of the antiferromagnet can be written in the form of:

$$E = -(\boldsymbol{M}_1 + \boldsymbol{M}_2)\boldsymbol{B} - \frac{1}{2} v_1 (M_1^2 + M_2^2) - v_2 \boldsymbol{M}_1 \boldsymbol{M}_2. \tag{6.70}$$

If a weak magnetic field is directed parallel to the magnetization of one of the sublattices and, accordingly, antiparallel to the second, then this is equivalent to the fact that the internal effective field acting in each of the sublattices becomes slightly different in magnitude, but due to the smallness of the external field, this does not affect the values and direction of magnetization. Thus, the susceptibility of the system with respect to the parallel field $\chi_\parallel = 0$ at $T = 0$. This susceptibility becomes nonzero at nonzero temperatures due to thermal fluctuations. Let's consider a more interesting case when the external field is applied perpendicular to the initial direction, along which the magnetization of both sublattices is aligned.

Let's assume that $|\boldsymbol{M}_1| = |\boldsymbol{M}_2| = M$. The external field tends to align the magnetizations along with the direction of

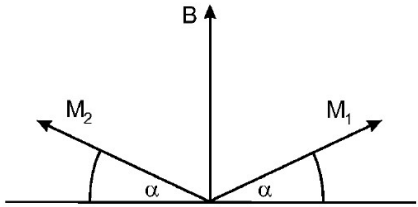

Figure 6.14: The canting of the magnetizations of the sublattices to the direction of the external field in the case of a perpendicular orientation of the field and the initial direction of the magnetizations. From [5].

the field, and the exchange interaction tends to keep them in an antiparallel state. As a result of the competition of these factors, it is possible to establish a state in which both magnetizations form a certain angle with their initial position. For symmetry reasons, these angles should be the same. Let's denote them α, see Fig. 6.14. It is possible to investigate the energy profitability of such a state and find the value of the angle α from the equation (6.70). For the configuration shown in Fig. 6.14 the energy is equal to:

$$E_\perp = -2MB\sin\alpha - v_1M^2 + v_2M^2\cos 2\alpha. \qquad (6.71)$$

From the condition $dE_\perp/d\alpha = 0$ we obtain

$$\cos\alpha(B + 2v_2M\sin\alpha) = 0, \qquad (6.72)$$

then it can found that the energy minimum corresponds to

$$\sin\alpha = -\frac{B}{2v_2M}, \quad 0 \le B \le -2v_2M,$$
$$\cos\alpha = 0, \quad B \ge -2v_2M. \qquad (6.73)$$

Thus, a non-zero value of the magnetization of the antiferromagnet arises along the direction of the field, i.e. perpendicular to the initial direction of the sublattice magnetizations.

This value is equal to

$$M_\perp = 2M\sin\alpha = -\frac{B}{v_2}, \quad 0 \le B \le -2v_2M,$$
$$M_\perp = 2M, \quad B \ge -2v_2M. \tag{6.74}$$

The corresponding susceptibility of an antiferromagnet in a perpendicular field is

$$\chi_\perp = \frac{dM_\perp}{dB} = -\frac{1}{v_2}. \tag{6.75}$$

This value coincides with the susceptibility at the Néel temperature. We have found that the susceptibility of the antiferromagnet at $T < T_N$ is anisotropic. For polycrystalline samples, for which different directions of the Néel vector (sublattice magnetization) in different domains are equally probable, susceptibility is obtained as a result of averaging:

$$\chi_{poly} = \frac{1}{3}\chi_\parallel + \frac{2}{3}\chi_\perp. \tag{6.76}$$

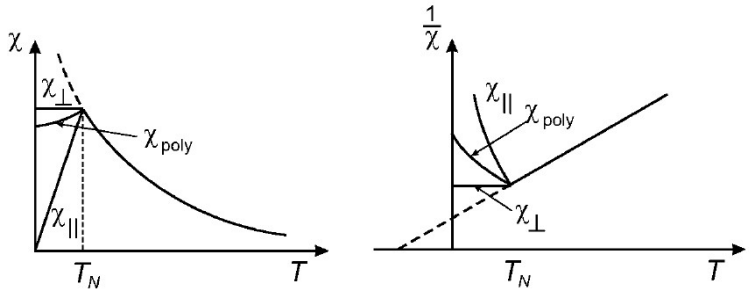

Figure 6.15: Temperature dependences of magnetic susceptibility and reverse magnetic susceptibility. From [5].

The qualitative behavior of all $\chi_\parallel$, $\chi_\perp$ и χ_{poly} susceptibilities depending on temperature is shown in Fig. 6.15.

6.5 Spiral magnetic order. Homework taks.

Spiral magnetic order often occurs in rare earth metals, which have a layered structure. These materials are characterized by ferromagnetic ordering within each layer, but the magnetization directions of two adjacent layers form an angle θ, see Fig. 6.16.

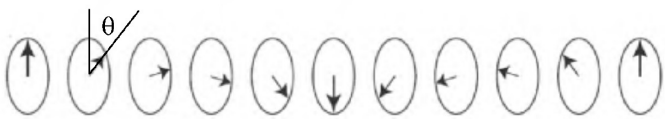

Figure 6.16: Spiral magnetic order. Within each layer there is ferromagnetic ordering, leading to the appearance of uniform magnetization. The magnetization vectors of adjacent layers make an angle θ with each other.

To describe the spiral magnetic order, we consider the model Heisenberg Hamiltonian, which takes into account the interaction between the nearest neighboring layers with the exchange integral J_1 and the next nearest neighboring layers with the exchange integral J_2. Each layer is described by a spin $\boldsymbol{S}_i$. Within the framework of classical consideration, the corresponding energy has the form:

$$E = -\sum_{ij} J_{ij} \boldsymbol{S}_i \boldsymbol{S}_j = -2NS^2(J_1 \cos\theta + J_2 \cos 2\theta), \quad (6.77)$$

where N is the number of layers, S is the absolute value of the spin of the layer, which is considered here as a classical vector.

It is obvious that at $J_1 > 0$ and $J_2 > 0$ interlayer ferromagnetic order is established in the system. But if J_1 and J_2 are of different signs, then the main state of the system is

not so obvious, because the tendency to establish, say, ferromagnetic ordering between nearby layers competes with the system's tendency to arrange its next nearest neighbors in an antiferromagnetic manner. This is the simplest example of a frustrated system.

By minimizing the energy of the system, obtain a phase diagram of the system states in the (J_1, J_2) plane. Identify regions of ferromagnetic, antiferromagnetic and helical ordering. Write equations for the boundaries of these areas.

6.6 The Heisenberg model beyond the mean field approximation. Magnons.

In general, the Hamiltonian of the Heisenberg model is written as:

$$\hat{H} = -\sum_{ij} J_{ij} \hat{\boldsymbol{S}}_i \hat{\boldsymbol{S}}_j \tag{6.78}$$

Let $J_{ij} = J \neq 0$ only for the nearest neighbors. The Heisenberg Hamiltonian can be written as:

$$\hat{H} = -J \sum_{ij} [\alpha(\hat{S}_i^x \hat{S}_j^x + \hat{S}_i^y \hat{S}_j^y) + \beta \hat{S}_i^z \hat{S}_j^z]. \tag{6.79}$$

Let D be the dimension of the spin vector. Then for $D = 1(\alpha = 0, \beta = 1)$ The Heisenberg Hamiltonian is called the Ising model. For for $D = 2(\alpha = 1, \beta = 0)$ is the XY-model. For the case $D = 3$, the name Heisenberg model is retained.

In addition to the dimension of the spin vector, there is also the dimension of the space d. The results produced by the described models depend significantly on the dimension of the space. Consider the Ising model.

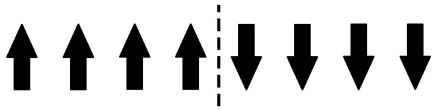

Figure 6.17: A one-dimensional Ising chain with a single defect.

The case of $D = 1, d = 1$ (one-dimensional Ising chain of $N + 1$ spins).

$$\hat{H} = -2J \sum_{i=1}^{N} \hat{S}_i^z \hat{S}_{i+1}^z, \quad J > 0 \tag{6.80}$$

In the ground state, all spins are lined up in parallel, the energy of the ground state $E_0 = -2JN\frac{1}{2}\frac{1}{2} = -\frac{1}{2}NJ$. Consider 1 defect, see Fig. 6.17. The energy of a system with a defect $E = E_0 + J$. The entropy of a system with a single defect is $S = k \ln N$. Therefore, $F = E - TS \to -\infty$ for $N \to \infty$ and $T \neq 0$. It follows that an ordered state cannot exist in this model at $T > 0$. That is, there is no phase transition, $T_c = 0$.

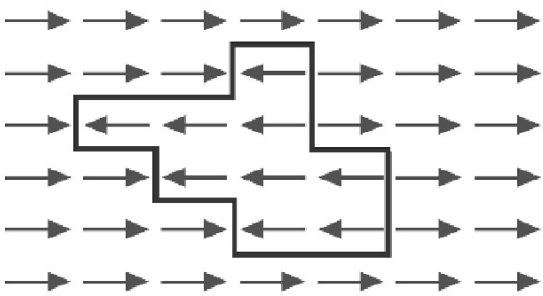

Figure 6.18: A defect in the two-dimensional Ising model. From [5].

The case of $D = 1, d = 2$ (two-dimensional Ising model). A possible defect is shown in Fig. 6.18. $E - E_0 \propto l$, where l is

the length of the defect boundary. The entropy also increases proportionally to the length of the boundary. This implies the advantage of an ordered state at $T < T_c$. There is a phase transition in the two-dimensional Ising model.

Exact solutions were obtained for the one-dimensional and two-dimensional Ising models.

6.6.1 The Heisenberg model. Spin waves.

The Heisenberg Hamiltonian in the external field has the form:

$$\hat{H} = -\frac{1}{2}\sum_{ij} J_{ij}\hat{\boldsymbol{S}}_i\hat{\boldsymbol{S}}_j - g\mu_B H\sum_i \hat{S}_{z,i}. \tag{6.81}$$

Ground state of the Hamiltonian:

$$|0\rangle = \prod_i |S\rangle_i = |S\rangle_1|S\rangle_2...|S\rangle_N. \tag{6.82}$$

To make sure that this is the eigen state of the Hamiltonian, we introduce the raising and lowering operators $\hat{S}_{\pm,i} = \hat{S}_{x,i} \pm i\hat{S}_{y,i}$.

$$\hat{S}_{\pm,i}|S_z\rangle_i = \sqrt{(S \mp S_z)(S + 1 \pm S_z)}|S_z \pm 1\rangle_i \tag{6.83}$$

Via the raising and lowering operators, the Hamiltonian can be written as:

$$\hat{H} = -\frac{1}{2}\sum_{ij} J_{ij}\hat{S}_{z,i}\hat{S}_{z,j} - g\mu_B H\sum_i \hat{S}_{z,i} - \frac{1}{2}\sum_{ij} J_{ij}\hat{S}_{-,i}\hat{S}_{+,j}. \tag{6.84}$$

Since $\hat{S}_{+,i}|S_{z,i}\rangle|_{S_{z,i}=S} = 0$, then $|0\rangle$ - is the eigenvector of Hamiltonian (6.84). The energy corresponding to this own state

$$E_0 = \langle 0|\hat{H}|0\rangle = -\frac{1}{2}S^2\sum_{ij} J_{ij} - Ng\mu_B HS. \tag{6.85}$$

It can be shown that E_0 is the minimum energy of the system (a task for an independent solution). It follows that $|0\rangle$ is the ground state of a ferromagnet.

Now let's find the low-lying excited states of the ferromagnet. At $T = 0$, the ferromagnet is in the ground state, all its spins are lined up in parallel, and the magnetization is equal to the saturation magnetization $M = g\mu_B nS$. At $T \neq 0$, to find the average magnetization, it is necessary to average the average magnetizations in all excited states with the Gibbs factor $e^{-E/T}$. To construct low-lying excited states, consider the state

$$|i\rangle = \frac{1}{\sqrt{2S}}\hat{S}_{-,i}|0\rangle. \tag{6.86}$$

This state corresponds to a spin projection reduced by 1 on the z axis at the i site. The action of the raising operator does not turn this state to zero $\hat{S}_{+,i}|i\rangle \neq 0$, and the action of the operator $\hat{S}_{-,j}\hat{S}_{+,i}$ moves the reduced spin from the site i to the site j:

$$\hat{S}_{-,j}\hat{S}_{+,i}|i\rangle = \frac{1}{\sqrt{2S}}\hat{S}_{-,j}\hat{S}_{+,i}\hat{S}_{-,i}|0\rangle = \\ \hat{S}_{-,j}\hat{S}_{+,i}|SSS...\underbrace{S-1}_{i}...SSS\rangle = \sqrt{2S}\hat{S}_{-,j}|0\rangle = 2S|j\rangle. \tag{6.87}$$

Therefore, the state $|i\rangle$ is not an eigenstate of the Heisenberg Hamiltonian. Besides,

$$\hat{S}_{z,j}|i\rangle = \begin{cases} S|i\rangle, & i \neq j, \\ (S-1)|i\rangle, & i = j. \end{cases} \tag{6.88}$$

Taking this into account we obtain:

$$\hat{H}|i\rangle = \Big(-\frac{1}{2}S^2\sum_{ij}J_{ij} - Ng\mu_B HS\Big)|i\rangle + g\mu_B H|i\rangle + S\sum_j J_{ij}\Big(|i\rangle - |j\rangle\Big) = E_0|i\rangle + g\mu_B H|i\rangle + S\sum_j J_{ij}\Big(|i\rangle - |j\rangle\Big), \quad (6.89)$$

this means that $|i\rangle$ is no longer an eigenstate of the Heisenberg Hamiltonian, but $\hat{H}|i\rangle$ is a linear combination of states in which the projection value of one of the spins has decreased by 1. We can find such a combination of states $|i\rangle$, which is a proper one for the Hamiltonian $\hat{H}$. You can search for it in the form

$$|k\rangle = \frac{1}{\sqrt{N}}\sum_l e^{ikl}|l\rangle. \quad (6.90)$$

It is necessary that $|k\rangle$ be an eigenstate of the Hamiltonian, i.e. that $\hat{H}|k\rangle = E_k|k\rangle$. Let's act with a Hamiltonian on the state $|k\rangle$:

$$\hat{H}|k\rangle = (E_0 + g\mu_B H)|k\rangle + \frac{S}{\sqrt{N}}\sum_{lj}J_{lj}e^{ikl}\Big(|l\rangle - |j\rangle\Big) = (E_0 + g\mu_B H)|k\rangle + S\sum_{l-j}J_{lj}\Big(1 - e^{ik(l-j)}\Big)|k\rangle. \quad (6.91)$$

Thus,

$$E_k = (E_0 + g\mu_B H) + 2S\sum_{i-j}J_{ij}\sin^2\frac{k(i-j)}{2}. \quad (6.92)$$

Energy, which is necessary to excite state $|k\rangle$ is:

$$\varepsilon_k = E_k - E_0 = g\mu_B H + 2S\sum_{i-j}J_{ij}\sin^2\frac{k(i-j)}{2}. \quad (6.93)$$

Now consider the physical interpretation of the state $|k\rangle$:

1) $|k\rangle$ - is a superposition of states with spin $NS-1$.

2) The probability of detecting a reduced spin value at the site i: $P_i = |\langle k|i\rangle|^2 = 1/N$, which implies that the reduced spin can equally likely belong to any magnetic ion.

3) Transverse correlation function:

$$\langle k|\hat{S}_\perp(i)\hat{S}_\perp(j)|k\rangle = \langle k|\hat{S}_{x,i}\hat{S}_{x,j} + \hat{S}_{y,i}\hat{S}_{y,j}|k\rangle = \frac{2S}{N}\cos[k(i-j)], \quad i \neq j. \tag{6.94}$$

Therefore, any spin has a small transverse component, on average equal to $\sqrt{2S/N}$, the orientations of the transverse components of the two spins at a distance of $i-j$ make up the angle $k(i-j)$.

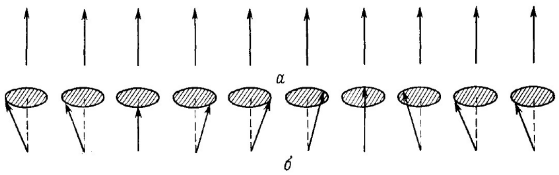

Figure 6.19: (a) A chain of spins in the ferromagnetic state; (b) in the spin wave state. From [8].

The magnetization distribution in the $|k\rangle$ state is shown in Fig. 6.19. This is a state with a spin wave or a magnon with a wave vector k and energy ε_k. Such single-magnon states are the exact eigenstates of the Heisenberg Hamiltonian. When calculating low-temperature properties, it is often assumed that higher-lying excited states of the Hamiltonian can be constructed as multimagnon states with an energy equal to the sum of the energies of individual magnons. For photons in a harmonic crystal, such states, as well as single-photon ones, are the exact eigenstates of the Hamiltonian, but for spin waves

this is only approximate due to the interaction of magnons. However, a multimagnon approximation (when higher excited states are assumed to have energy $\varepsilon_{k1} + \varepsilon_{k2} + ... + \varepsilon_{kN}$) is used and correctly reproduces the basic term of magnetization at low temperatures. Therefore, we will use it to calculate $M(T)$.

Since each spin wave reduces the total spin of the system by 1, the magnetization of the system at low temperature T has the form:

$$M(T) = M(0)\Big[1 - \frac{1}{NS}\sum_k n_k\Big], \tag{6.95}$$

where $n_k = 1/(e^{\varepsilon_k/kT} - 1)$ is the average number of magnons with the wave vector k. At low temperatures, only spin waves with low energy are excited, so $k \ll 1$ and then

$$\varepsilon_k \approx \frac{S}{2}\sum_{i-j} J_{ij}k^2(i-j)^2 \propto k^2. \tag{6.96}$$

Cosequently $d\varepsilon/dk \propto k \propto \sqrt{\varepsilon}$.

$$\sum_k n_k = \int \frac{d^3k}{(2\pi)^3}\frac{1}{e^{\varepsilon_k/kT}-1} = \frac{4\pi}{(2\pi)^3}\int \frac{k^2dk}{e^{\varepsilon_k/kT}-1} = \frac{1}{2\pi^2}\int \frac{k^2 d\varepsilon \frac{1}{d\varepsilon/dk}}{e^{\varepsilon/kT}-1} = \int \frac{g(\varepsilon)d\varepsilon}{e^{\varepsilon/kT}-1}, \tag{6.97}$$

where $g(\varepsilon) \propto \sqrt{\varepsilon}$. Thus,

$$\sum_k n_k = A\int_0^\infty (kT)^{3/2}\frac{\sqrt{x}dx}{e^x - 1} \propto T^{3/2}. \tag{6.98}$$

Therefore, for low-temperature magnetization we obtain

$$\frac{M(T)}{M(0)} = 1 - cT^{3/2}. \tag{6.99}$$

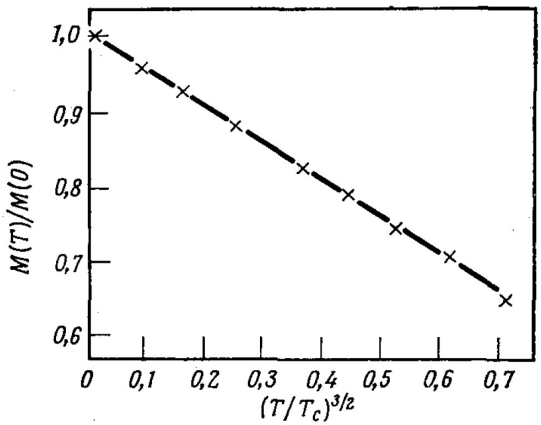

Figure 6.20: Dependence of the ratio of the spontaneous magnetization of gadolinium ($T_c = 293K$) to the saturation magnetization at $T = 0$ from $(T/T_c)^{3/2}$. From [8].

This expression is called the Bloch law of $T^{3/2}$. The law of $T^{3/2}$ is well confirmed by the results of experiments in isotropic ferromagnets, see Fig. 6.20.

Thus, magnons make a significant contribution to the magnetization of the magnet, leading to a cardinal difference between the magnetization at low temperatures and the mean field model, in which the difference between the magnetization and its value at zero temperature turns out to be exponentially suppressed, see the formula (6.42). Magnons have an even more drastic effect on magnetization in two-dimensional and one-dimensional cases. In the 1D and 2D Heisenberg models, the magnetization is zero at any temperature $T > 0$, i.e. ferromagnetism does not exist. This statement is called the Mermin-Wagner theorem. The reason for the absence of spontaneous magnetization is that the number of low-energy magnons that can be excited at arbitrarily low temperatures diverges and they destroy any magnetic order. Let's show this

in the case of $d = 2$.

$$\sum_k n_k^{2D} = \int \frac{d^2k}{(2\pi)^2} \frac{1}{e^{\varepsilon_k/kT} - 1} \propto \int \frac{kdk}{e^{\varepsilon_k/kT} - 1} \propto$$

$$\int \frac{kd\varepsilon \frac{1}{d\varepsilon/dk}}{e^{\varepsilon/kT} - 1} \propto \int \frac{d\varepsilon}{e^{\varepsilon/kT} - 1}. \quad (6.100)$$

Thus,

$$\sum_k n_k \propto \int_0^\infty \frac{dx}{e^x - 1}, \quad (6.101)$$

which diverges logarithmically at the lower limit. However, 2D ferromagnets and antiferromagnets exist and in recent years this field of physics has been rapidly developing, many relevant materials have been discovered, which are obtained mainly by separating monolayers from van der Waals layered crystals [9]. The point here is that the divergence of the low-temperature magnon number in 2D is essentially based on the gapless nature of the magnon spectrum in the isotropic Heisenberg model (6.96), i.e. based on the fact that magnons can be excited at arbitrarily close to zero energies. In fact, all two-dimensional materials are in a three-dimensional environment (lying on a substrate), which causes anisotropy of their properties. In the anisotropic case, magnetic moments cannot rotate in any direction with an infinitesimal change in energy. As a result, a gap opens in the magnon spectrum

$$\varepsilon_k = \Delta + Bk^2, \quad (6.102)$$

which leads to the fact that the number of magnons excited at low temperatures becomes finite:

$$\sum_k n_k^{2D,an} \propto \int_\Delta^\infty \frac{d\varepsilon}{e^{\varepsilon/kT} - 1}. \quad (6.103)$$

This result provides the possibility of the appearance of ferromagnetism in 2D systems at $T > 0$.

6.7 Anisotropic Heisenberg model. Homework task.

Consider anisotropic Heisenberg Hamiltonian

$$\hat{H} = -\frac{1}{2}\sum_{ij}\Big[J_{z,ij}\hat{S}_{z,i}\hat{S}_{z,j} + J_{ij}(\hat{S}_{x,i}\hat{S}_{x,j} + \hat{S}_{y,i}\hat{S}_{y,j})\Big],$$

where $J_{z,ij} > J_{ij}$. Show that the ground state and the state with one spin wave, constructed in the lecture, remain the eigenstates of this Hamiltonian, but the excitation energies of spin waves increase by a certain amount (a gap in the spectrum). Find it. Show that spontaneous magnetization at low temperatures differs from saturation magnetization by an exponential value depending on $-1/T$.

Chapter 7

Magnetic anisotropy.

Previously, only magnetically isotropic systems were considered, for which the free energy does not depend on the direction of magnetization $F = F(|\boldsymbol{M}|)$. In particular, for the isotropic Heisenberg Hamiltonian, the energy levels do not depend on the direction of $\boldsymbol{M}$. Real magnetic materials are not isotropic. Magnetic anisotropy can have various physical causes. The most important classes of magnetic anisotropies are listed below:

1. Magnetocrystalline anisotropy - the magnetization is oriented along certain axes in the crystal.

2. Shape anisotropy - the direction of magnetization is determined by the shape of the sample.

3. Induced magnetic anisotropy - certain directions of magnetization can be stabilized by temporarily placing the sample in a magnetic field.

4. Magnetostriction - anisotropy associated with spontaneous deformation of the sample.

5. Surface anisotropy

7.1 Magnetocrystalline anisotropy.

This type of anisotropy is caused by the spin-orbit interaction of $E \propto \boldsymbol{LS}$. After averaging, the electronic orbitals are elongated along certain axes in the crystal, and there are preferable directions for the orbital moment. Therefore, the magnetization determined by the spin moment also tends to lie along the crystal axes. The spin-orbit interaction can be calculated from first principles, but it is simpler to use a phenomenological approach. Within the framework of this approach, a phenomenological expression is written for the contribution to the free energy of the system, based on symmetric considerations.

We introduce the direction cosines of the magnetization vector:

$$\alpha_1 = \frac{M_x}{M} = \sin\theta\cos\phi, \tag{7.1}$$

$$\alpha_2 = \frac{M_y}{M} = \sin\theta\sin\phi, \tag{7.2}$$

$$\alpha_3 = \frac{M_z}{M} = \cos\theta, \tag{7.3}$$

where θ is the polar angle and ϕ is the azimuthal angle of the spherical coordinate system. $\alpha_1^2 + \alpha_2^2 + \alpha_3^2 = 1$. The energy of magnetic anisotropy can be decomposed in a series according to the components of magnetization (direction cosines):

$$E_{crys} = E_0 + \sum_i b_i\alpha_i + \sum_{ij} b_{ij}\alpha_i\alpha_j + \sum_{ijk} b_{ijk}\alpha_i\alpha_j\alpha_k + \sum_{ijkl} b_{ijkl}\alpha_i\alpha_j\alpha_k\alpha_l + ... \tag{7.4}$$

The anisotropy energy does not depend on the change in the sign of magnetization $E(\boldsymbol{M}) = E(-\boldsymbol{M})$, which implies that the coefficients before the odd degrees of the direction cosines

are zero. Further meaningful advances can be obtained for specific crystallographic systems.

7.1.1 Cubic crystal symmetry.

Due to the symmetry of $E(\alpha_i) = E(-\alpha_i)$, it follows that the terms $\propto \alpha_i\alpha_j$ with $i \neq j$ are zero, and, in general, the terms in which α_i is contained in any odd degree are also zero. Moreover, for cubic symmetry, all three crystal axes x, y, z aligned with the edges of the cube are equivalent. Therefore, $b_{11} = b_{22} = b_{33}$, which gives

$$\sum_{ij} b_{ij}\alpha_i\alpha_j = b_{11}(\alpha_1^1 + \alpha_2^2 + \alpha_3^2) = b_{11}, \tag{7.5}$$

$$\sum_{ijkl} b_{ijkl}\alpha_i\alpha_j\alpha_k\alpha_l = b_{1111}(\alpha_1^4 + \alpha_2^4 + \alpha_3^4) + 6b_{1122}(\alpha_1^2\alpha_2^2 + \alpha_1^2\alpha_3^2 + \alpha_2^2\alpha_3^2). \tag{7.6}$$

Taking into account (7.5) and (7.6), from (7.4) we obtain:

$$E_{crys} = E_0 + b_{11} + b_{1111}(\alpha_1^4 + \alpha_2^4 + \alpha_3^4) + 6b_{1122}(\alpha_1^2\alpha_2^2 + \alpha_1^2\alpha_3^2 + \alpha_2^2\alpha_3^2) + ..., \tag{7.7}$$

taking into account $1 = (\alpha_1^1 + \alpha_2^2 + \alpha_3^2)^2 = \alpha_1^4 + \alpha_2^4 + \alpha_3^4 + 2(\alpha_1^2\alpha_2^2 + \alpha_1^2\alpha_3^2 + \alpha_2^2\alpha_3^2)$ it can be rewritten as:

$$E_{crys}^{cubic} = K_0 + K_1(\alpha_1^2\alpha_2^2 + \alpha_1^2\alpha_3^2 + \alpha_2^2\alpha_3^2) + K_2\alpha_1^2\alpha_2^2\alpha_3^2 + ... \tag{7.8}$$

Let's look at how energy surfaces look depending on the direction in a cubic crystal. For the main crystallographic directions in a cubic crystal (see Fig. 7.1) we have:

$$[100]: \quad \alpha_1 = 1, \alpha_2 = \alpha_3 = 0$$
$$E_{100} = K_0, \tag{7.9}$$

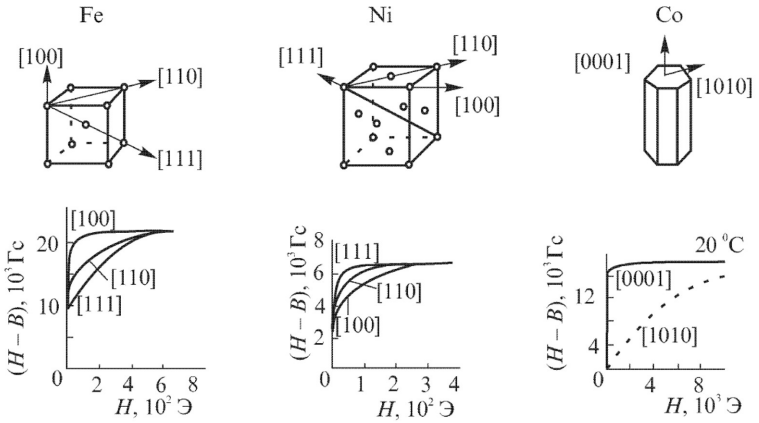

Figure 7.1: Top row: the main crystallographic directions for cubic symmetry crystals (Fe,Ni) and hexagonal symmetry crystals (Co). Bottom row: The magnetization curves of the corresponding single crystals along the main crystallographic directions. From [7].

$$[110]: \quad \alpha_1 = \alpha_2 = 1/\sqrt{2}, \alpha_3 = 0$$
$$E_{110} = K_0 + \frac{1}{4}K_1, \tag{7.10}$$

$$[111]: \quad \alpha_1 = \alpha_2 = \alpha_3 = 1/\sqrt{3},$$
$$E_{111} = K_0 + \frac{1}{3}K_1 + \frac{1}{27}K_2. \tag{7.11}$$

The values of the anisotropy constants for single crystals of Fe, Ni and Co are shown in the table in Fig. 7.2. The table shows that the most important constant is K_1. Considering only this constant, we obtain that for $K_1 > 0$, the direction [100] is the axis of easy magnetization, and the direction [111] is the heavy axis. An example of the relevant material is Fe.

		bcc-Fe	fcc-Ni	hcp-Co
K_1	[J/m^3]	$5.48 \cdot 10^4$	$-12.63 \cdot 10^4$	$7.66 \cdot 10^5$
	[eV/atom]	$4.02 \cdot 10^{-6}$	$-8.63 \cdot 10^{-6}$	$5.33 \cdot 10^{-5}$
K_2	[J/m^3]	$1.96 \cdot 10^2$	$5.78 \cdot 10^4$	$1.05 \cdot 10^5$
	[eV/atom]	$1.44 \cdot 10^{-8}$	$3.95 \cdot 10^{-6}$	$7.31 \cdot 10^{-6}$
K_3	[J/m^3]	$0.9 \cdot 10^2$	$3.48 \cdot 10^3$	–
	[eV/atom]	$6.6 \cdot 10^{-9}$	$2.38 \cdot 10^{-7}$	–

Figure 7.2: The magnetocrystalline anisotropy constants for Fe, Ni and Co at $T = 4.2K$. From [5].

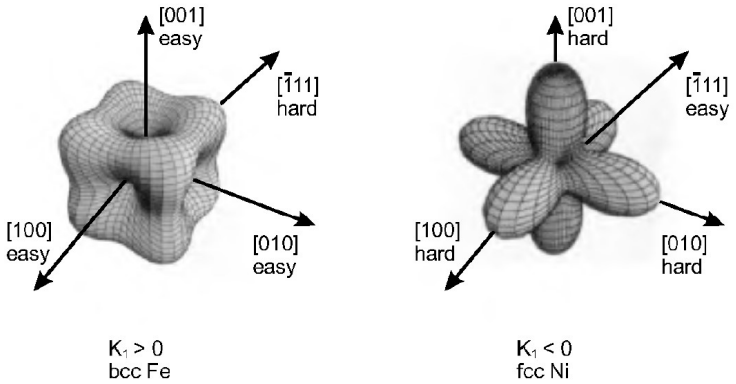

Figure 7.3: Energy surfaces. From [5].

On the contrary, for $K_1 < 0$, the direction [111] is the axis of easy magnetization, and the direction [100] is the heavy axis. An example is Ni. The energy surfaces for Fe and Ni are shown in Fig. 7.3. The value of the anisotropy constant also determines the rate at which saturation magnetization is achieved when the sample is magnetized in a field of a certain direction. The corresponding magnetization curves are shown for Fe, Ni and Co in the lower row in Fig. 7.1.

If the constants K_1 and K_2 are of the same order of magnitude, as sometimes happens (for example, for Ni in a certain

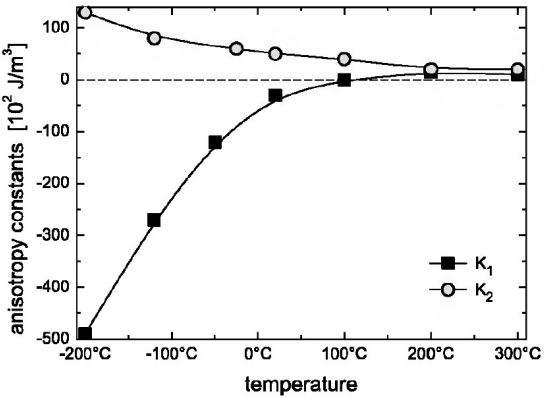

Figure 7.4: Температурная зависимость констант магнитокристаллической анизотропии для Ni. Из книги [5].

temperature range), then taking into account K_2 can greatly change the picture of the magnetic anisotropy energy. For example, the [110] direction can become both a easy and a heavy axis. The anisotropy constants depend significantly on temperature, see Fig. 7.4, including the directions of the easy and heavy axes may change with temperature changes.

7.1.2 Tetragonal and hexagonal symmetry of the crystal.

Tetragonal symmetry. As in the case of a cubic crystal, $E(\alpha_i) = E(-\alpha_i)$, which implies that the terms $\propto \alpha_i\alpha_j$ with $i \neq j$ vanish. But in this case, the symmetry of the crystal decreases because one of the crystal axes is not equivalent to the other two. Therefore, only the indices $i = 1$ and 2 are indistinguishable. In this case

$$\sum_{ij} b_{ij}\alpha_i\alpha_j = b_{11}(\alpha_1^2 + \alpha_2^2) + b_{33}\alpha_3^2. \tag{7.12}$$

Using $\alpha_1^1 + \alpha_2^2 = 1 - \alpha_3^2$, from (7.12) we get

$$\sum_{ij} b_{ij}\alpha_i\alpha_j = b_{11} + (b_{33} - b_{11})\alpha_3^2 = a_0 + a_1\alpha_3^2. \qquad (7.13)$$

$$\sum_{ijkl} b_{ijkl}\alpha_i\alpha_j\alpha_k\alpha_l = b_{1111}(\alpha_1^4 + \alpha_2^4) + b_{3333}\alpha_3^4 + 6b_{1122}\alpha_1^2\alpha_2^2 + 12b_{1133}\alpha_3^2(\alpha_1^2 + \alpha_2^2). \qquad (7.14)$$

Substituting (7.13) and (7.14) into(7.4), получим:

$$E_{crys}^{tetra} = K_0 + K_1\alpha_3^2 + K_2\alpha_3^4 + K_3(\alpha_1^4 + \alpha_2^4) + ... = K_0 + K_1\cos^2\theta + K_2\cos^4\theta + K_3\sin^4\theta(\sin^4\phi + \cos^4\phi) = K_0' + K_1'\sin^2\theta + K_2'\sin^4\theta + K_3'\sin^4\theta\cos 4\phi + ... \qquad (7.15)$$

The term $\propto \cos 4\phi$ reflects the presence of a 4th order symmetry axis.

Hexagonal symmetry. Let us present without derivation the expression for the anisotropy energy of a hexagonal crystal:

$$E_{crys}^{hex} = K_0 + K_1\sin^2\theta + K_2\sin^4\theta + K_3\sin^6\theta + K_4\sin^6\theta\cos 6\phi + ... \qquad (7.16)$$

From (7.15) and (7.16) it is clear that E_{crys}^{tetra} has cylindrical symmetry up to second order in $\sin\theta$, and E_{crys}^{hex} up to 4th order. Up to these orders of accuracy (as a rule, such accuracy is sufficient for good agreement with experiment), tetragonal and hexagonal crystals are equivalent to crystals with single-axis magnetic anisotropy.

So, for tetragonal and hexagonal crystals

$$E_{crys} = K_0 + K_1\sin^2\theta + K_2\sin^4\theta. \qquad (7.17)$$

When $K_1 > 0$ and $K_2 > 0$ [001] is the easy axis. This is called an easy-axis type magnet. When $K_1 < 0$ and $K_2 < 0$ [001] is

a hard axis. The magnetization tends to lie in the xy plane and such a magnet is called an easy-plane type magnet. If one of the constants is positive and the other is negative, then at $\sin^2\theta = -K_1/2K_2$, a magnetic transition from one type to another occurs.

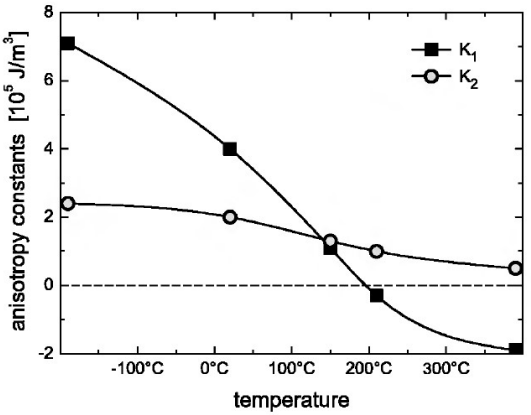

Figure 7.5: Temperature dependence of the magnetocrystalline anisotropy constants for Co. From [5].

An example of a uniaxial crystal of the easy-axis type can be Co at low temperature, see the table in Fig. 7.2. At high temperatures $\sim 500-600K$, Co transitions from the easy-axis type to the easy-plane type due to the temperature dependence of the anisotropy constants, see Fig. 7.5.

7.2 Shape anisotropy.

Polycrystals without a preferred orientation of granules do not have magnetocrystalline anisotropy. However, if the sample is not spherical, one or more easy axes arise, determined by the shape. This effect is due to the magnetic dipole-dipole interaction of the magnetization vectors in different parts of

the sample. Indeed, in the simplest example of the interaction of two dipoles

$$U = -\frac{\boldsymbol{\mu}_1 \boldsymbol{B}_1}{2} - \frac{\boldsymbol{\mu}_2 \boldsymbol{B}_2}{2} = \frac{\mu_0}{4\pi}\Big(\frac{\boldsymbol{\mu}_1 \boldsymbol{\mu}_2}{r^3} - \frac{3(\boldsymbol{\mu}_1 \boldsymbol{r})(\boldsymbol{\mu}_2 \boldsymbol{r})}{r^5}\Big) \quad (7.18)$$

It can be seen that the energy of the interaction depends on the relative position of the magnetic moments and their orientation relative to the axis connecting them. For example, $(\mu_0/4\pi)\mu_1\mu_2/r^3$ (in unstable configuration $\uparrow\uparrow$) or $-(\mu_0/2\pi)\mu_1\mu_2/r^3$ (in stable configuration $\rightarrow\rightarrow$). For a ferromagnet, which can be represented as a set of dipoles, the energy of the dipole-dipole interaction has the form:

$$U = -\frac{1}{2}\sum_i \sum_{i \neq j} \boldsymbol{\mu}_i \boldsymbol{B}_i =$$

$$-\frac{1}{2}\sum_i \boldsymbol{\mu}_i \sum_{i \neq j} \frac{\mu_0}{4\pi}\Big(\frac{3(\boldsymbol{\mu}_i \boldsymbol{r}_{ij})\boldsymbol{r}_{ij}}{r_{ij}^5} - \frac{\boldsymbol{\mu}_i}{r_{ij}^3}\Big). \quad (7.19)$$

Turning to the integral in this expression, we get:

$$U = -\frac{1}{2}\int d^3 r \boldsymbol{M}(\boldsymbol{r}) \int d^3 r' \boldsymbol{B}(\boldsymbol{r}, \boldsymbol{r}'), \quad (7.20)$$

where

$$B(\boldsymbol{r}, \boldsymbol{r}') = \frac{\mu_0}{4\pi}\Big(\frac{3[\boldsymbol{M}(\boldsymbol{r}')(\boldsymbol{r} - \boldsymbol{r}')](\boldsymbol{r} - \boldsymbol{r}')}{|\boldsymbol{r} - \boldsymbol{r}'|^5} - \frac{\boldsymbol{M}(\boldsymbol{r}')}{|\boldsymbol{r} - \boldsymbol{r}'|^3}\Big). \quad (7.21)$$

This expression contains a divergence inside the body, so when calculating the magnetic field $\boldsymbol{B}(\boldsymbol{r})$ we use the following technique:

$$B(\boldsymbol{r}) = \int\limits_{\Omega} d^3 r' \boldsymbol{B}(\boldsymbol{r}, \boldsymbol{r}') + \sum_{j \in \omega} \boldsymbol{B}_{ij}, \quad (7.22)$$

where ω is a sphere of radius R around the magnetic moment $\boldsymbol{m}_i$ (Lorentz sphere), and Ω is the rest of the volume of the

body without the Lorentz sphere. The radius of the Lorentz sphere is chosen much smaller than the characteristic scale of the magnetization change, but much larger than the interatomic distance.

Inside a material we have $\boldsymbol{B} = \mu_0(\boldsymbol{H}+\boldsymbol{M})$. From Maxwell's equation we get:

$$\boldsymbol{\nabla} B = 0 \Rightarrow \boldsymbol{\nabla} H = -\boldsymbol{\nabla}\boldsymbol{M} = \rho_M, \tag{7.23}$$

which, together with the second Maxwell equation $rot\boldsymbol{H} = 0$, defines the standard electrostatic problem for the field $\boldsymbol{H}$ for a given magnetic charge distribution $\rho_M = -\boldsymbol{\nabla}\boldsymbol{M}$. The solution of this problem has the form:

$$\boldsymbol{H}(\boldsymbol{r}) = -\frac{1}{4\pi}\int\limits_{\Omega} d^3r' \frac{[\boldsymbol{\nabla}'\boldsymbol{M}(\boldsymbol{r}')(\boldsymbol{r}-\boldsymbol{r}')]}{|\boldsymbol{r}-\boldsymbol{r}'|^3}. \tag{7.24}$$

Thus, in a finite sample the volume relation $\boldsymbol{B} = \mu_0\boldsymbol{M}$ stops working and magnetic charges appear on its surface, which create stray fields outside the sample and a "demagnetizing" field $\boldsymbol{H}$ inside the sample, which is not aligned with the magnetization and leads to a dependence of the energy of the dipole-dipole interaction from the direction of magnetization.

The term $\sum\limits_{j\in\omega} \boldsymbol{B}_{ij}$ in Eq. (7.22) disappears for a cubic lattice, and for a non-cubic one it can be included in the magnetocrystalline anisotropy, because it does not depend on the shape of the sample. Then we get that the anisotropy energy of the shape has the form:

$$U = -\frac{\mu_0}{2}\int d^3r \boldsymbol{M}\boldsymbol{H}. \tag{7.25}$$

All terms of $\propto \int d^3r M^2$, and therefore independent of the direction of magnetization of the sample, are omitted here. Calculating the demagnetization field $\boldsymbol{H}$ for samples of arbitrary

shape is a rather difficult task. But for uniformly magnetized ellipsoidal samples, the demagnetization field is also homogeneous and has the form:

$$H_i = -N_{ij} M_j, \tag{7.26}$$

where the matrix $\hat{N}$ with components N_{ij} is a demagnetization tensor. $Tr\hat{N} = 1$. Then the shape anisotropy energy (also called the energy of stray fields or the energy of the dipole-dipole interaction) takes the form:

$$U = \frac{\mu_0}{2} \int d^3 r (\boldsymbol{M})^T \hat{N} \boldsymbol{M}. \tag{7.27}$$

The energy of stray fields is always positive. If we select the coordinate axes along the main axes of the ellipsoid a, b, c, then the demagnetization tensor acquires a diagonal structure and the energy of the stray fields can be written as:

$$E_{str} = U = \frac{\mu_0}{2} M^2 V \Big(N_a \alpha_a^2 + N_b \alpha_b^2 + N_c \alpha_c^2 \Big). \tag{7.28}$$

In the case of sphere, the demagnetization tensor is isotropic $N_i = 1/3$ for $i = a, b, c$ and all directions of magnetization are energetically equivalent.

For rotational ellipsoid, i.e. a body having symmetry with respect to rotation around the c axis:

$$N_a = N_b, \quad N_c = 1 - 2N_a, \tag{7.29}$$

$$E_{str} = \frac{\mu_0}{2} M^2 V \Big(N_a \sin^2\theta + (1 - 2N_a) \cos^2\theta \Big) = \frac{\mu_0}{2} M^2 V \Big(N_a + (1 - 3N_a) \cos^2\theta \Big). \tag{7.30}$$

For infinitely long cylinder $N_a = N_b = 1/2$, $N_c = 0$.

$$E_{str} = \frac{\mu_0}{4} M^2 V \sin^2\theta. \tag{7.31}$$

For infinite flat plate $N_a = N_b = 0$, $N_c = 1$.

$$E_{str} = \frac{\mu_0}{2} M^2 V \cos^2\theta. \tag{7.32}$$

This result is very important for thin films and multilayers. For them, if we write

$$E_{str} = K_0 + K_{shape} \sin^2\theta, \tag{7.33}$$

then $K_{shape} \propto M^2 < 0$. In addition, the shape anisotropy usually dominates the magnetocrystalline anisotropy. Therefore, in films, the magnetization lies in the plane of the film.(a) Random distribution of atoms in a binary alloy; (b) ideal isotropic long-range order; (c) anisotropic short-range order with a preferred bond direction, formed as a result of annealing in a magnetic field.

7.3 Induced magnetic anisotropy.

For magnetic alloys having a cubic crystal structure, uniaxial anisotropy can be achieved by annealing in a magnetic field. The necessary ingredients for this are the chaotic arrangement of atoms of various substances in the alloy lattice and high critical temperatures, which allow the atoms to exchange places in the crystal lattice through thermal diffusion.

The mechanism for the formation of induced single-axis anisotropy is as follows. The magnetic field orients the magnetization at $T < T_c$. The binding energy of two neighboring atoms in a magnetized crystal depends on the angle between the straight line connecting the atoms and the direction of magnetization $E \propto l \cos^2\phi$, where ϕ is the angle between the straight line connecting the atoms and the direction of magnetization and l is a constant depending on the type of bond (in a binary alloy AA, AB or BB) and temperature. A pair

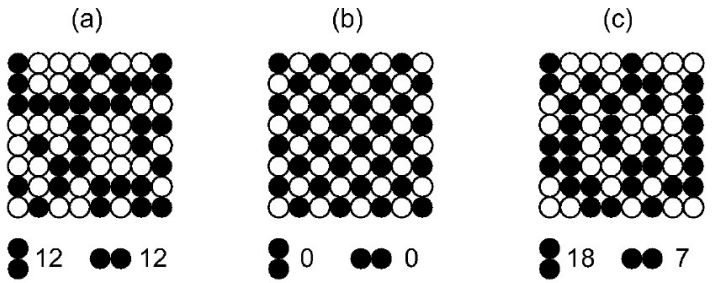

Figure 7.6: (a) Random distribution of atoms in a binary alloy; (b) ideal isotropic long-range order; (c) anisotropic short-range order with a preferred bond direction, formed as a result of annealing in a magnetic field. From [5].

of atoms forming a bond tends to extend the axis along or across the magnetization, depending on the sign of l. If the temperature is high and diffusion of atoms is possible, then the atoms are rearranged in the field so as to minimize this energy. This process is illustrated by the transition from Fig. 7.6(a) to Fig. 7.6(c). When cooled in a field, this order is frozen, resulting in uniaxial anisotropy.

7.4 Magnetostriction.

Until now, the crystal lattice was considered rigid. Let us introduce an elastic degree of freedom.

For a cubic lattice, the energy of magnetocrystalline anisotropy has the form $E_{crys}^{cubic} = K_1^{cubic} \cdot O(\alpha^4)$, and for tetragonal anisotropy $E_{crys}^{tetra} = K_1^{tetra} \cdot O(\alpha^2) = K_1^{tetra} \sin^2\theta$. As a rule, $K_1^{tetra} > K_1^{cubic}$, so lattice deformation that transforms the crystal from cubic to tetragonal symmetry is beneficial. This deformation is limited by elastic energy. In the simplest case, when deformation is possible along one axis, the energy of the system,

including the contribution of the energy of tetragonal magnetic anisotropy (we neglect cubic anisotropy in comparison with tetragonal and elastic energies), has the form:

$$E = K_1\varepsilon(1-\alpha_3^2) + \frac{c\varepsilon^2}{2}, \tag{7.34}$$

where ε is the relative change in length along a given direction. For a fixed direction of magnetization, the minimum energy of the system is achieved at

$$\varepsilon = -\frac{K_1}{c}(1-\alpha_3^2). \tag{7.35}$$

Substituting this value into (7.34), we get:

$$E = -\frac{K_1^2}{2c}(1-\alpha_3^2)^2, \tag{7.36}$$

that is, magnetostrictive deformation leads to the appearance of uniaxial anisotropy of the easy plane type. In the general case, it is necessary to introduce a deformation tensor and an elasticity tensor. One or more easy axes may also appear in a crystal as a result of magnetostrictive deformations. The characteristic values of magnetostrictive strain are of the order of $\varepsilon \sim 10^{-5}$.

7.5 Surface anisotropy.

Until now, all types of anisotropy have been associated with the bulk properties of crystals. For low-dimensional systems, the contribution to the anisotropy energy associated with the presence of the sample surface also plays a significant role. In thin films, the effective anisotropy constant contains both a volume contribution, determined by the shape anisotropy energy, and a surface contribution ($E_{an} = K_{eff}\sin^2\theta$):

$$K_{eff} = K^V + 2K^S/d, \tag{7.37}$$

where K^V is the shape anisotropy constant, K^S is the surface anisotropy constant, d is the film thickness. As the film thickness increases, the contribution of surface anisotropy to the effective constant decreases $\propto 1/d$, which leads to the appearance of a corresponding factor in (7.37). The factor of 2 arises from the presence of 2 surfaces on the film.

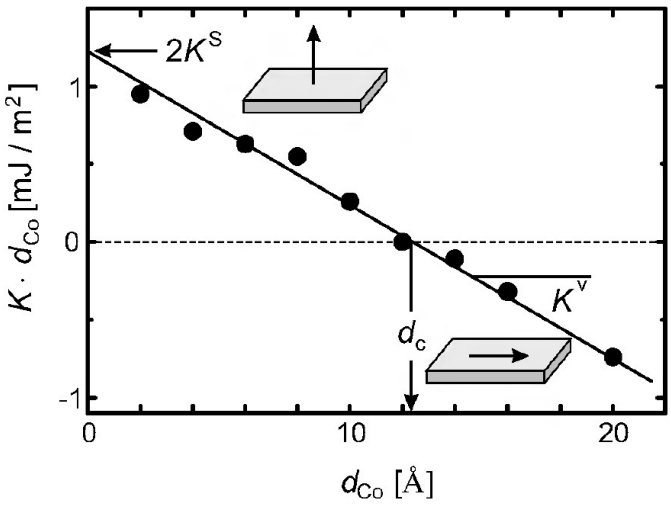

Figure 7.7: Magnetic anisotropy in a thin Co film in a Co/Pd multilayer as a function of Co film thickness. The slope of the line gives K^V, and the approximation of the linear function to $d_{Co} = 0$ gives $2K^S$. From [5].

The physical cause of surface anisotropy is again the spin-orbit interaction. Due to the breaking of symmetry with respect to inversion relative to the surface of the sample, an effective electric field arises near the surface, as a result of which the electron orbitals of surface atoms are extended along the normal to the surface. This causes the spin of the electron shell, as a rule, to also elongate along the normal, as a result of which K_S gives an anisotropy of the easy axis type

and leads to a change in the equilibrium orientation of magnetization from parallel to the film plane to perpendicular in ultrathin films at a critical film thickness $d_c = -2K^S/K^V$, see Fig. 7.7.

Chapter 8

Domain structure of magnets.

An unmagnetized ferromagnetic sample below T_c consists of domains - regions of uniform magnetization, the magnetization in each of which is directed along the easy axis of this domain. The magnetization of a macroscopic sample averaged over all domains is zero. The boundaries between neighboring domains are called domain walls. The domain concept explains many properties of magnetic materials. For example: (i) zero average magnetization of a non-magnetized magnet; (ii) the sufficiency of very weak magnetic fields $B \sim 10^{-6}T$ in soft magnetic materials to achieve magnetization $\mu_0 M \sim 1T$. This is explained by the fact that a weak external field does not reorient all magnetic moments, but only moves the domain walls.

8.1 Domain walls.

First of all, domain walls can be classified by the angle that the magnetizations of neighboring domains make with each

other. The most common are 180-degree and 90-degree walls, see Fig. 8.1. What type of domain wall is realized depends on the magnetocrystalline anisotropy:

1) Uniaxial anisotropy. An example is Co. - 180°-walls.

2) Triaxial material. An example is Fe. It has three easy axes along [100], [010] and [001] - 180° and 90° walls.

3) Quadriaxial material. An example is Ni. It has easy axes along [111] directions - 180°, 109° and 71° walls.

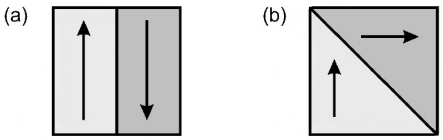

Figure 8.1: (a) 180°-domain wall; (b) 90°-domain wall. From [5].

The most common 180°-domain walls can be further divided into:

1) Bloch's walls, in which the rotation of the magnetization occurs in the plane of the wall;

2) Néel walls, in which the rotation of the magnetization occurs in a plane perpendicular to the plane of the wall.

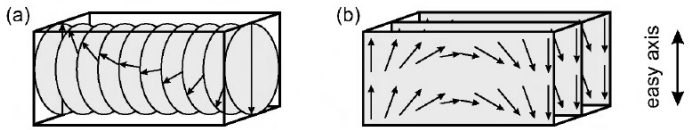

Figure 8.2: (a) Rotation of the magnetization of the Bloch wall; (b) rotation of the magnetization of the Neel wall. From [5].

The Bloch and Neel walls are shown in Fig. 8.2. Bloch walls are realized mainly in bulk crystals, since the magneti-

zation, which does not leave the plane of the domain interface, minimizes stray fields. Neel walls are realized in thin films, where, due to the anisotropy of the magnetization shape, it is not advantageous to go out of the film plane.

8.1.1 The width of the domain wall.

Let's consider how the width of the domain wall is determined and evaluate it. In the classical limit, the energy of the exchange interaction of two spins has the form:

$$E = -2J\boldsymbol{S}_1\boldsymbol{S}_2 = -2JS^2\cos\delta\varphi \approx -2JS^2 + JS^2\delta\varphi^2. \quad (8.1)$$

The last approximate equality is, of course, valid if the angle between the two spins is $\delta\varphi \ll 1$. Let N spins participate in the reversal of magnetization by π. Then $\delta\varphi = \pi/N$. Energy is required to flip one spin per π per N steps

$$E = NJS^2\delta\varphi^2 = \pi^2 JS^2/N. \quad (8.2)$$

There are $1/a^2$ spins per unit wall area, where a is a lattice constant. Therefore, the exchange contribution to the energy of the wall per unit area of the wall has the form:

$$E_{ex}^{w} = \frac{\pi^2 JS^2}{Na^2}. \quad (8.3)$$

This energy tends to stretch the wall, its minimum is reached at $N \to \infty$. However, it is also necessary to take into account the energy of the magnetocrystalline anisotropy, which tends to shorten the wall. The result of the competition of these two factors determines the final width of the wall. The energy of the magnetocrystalline (uniaxial) anisotropy per unit volume of the material has the form:

$$E_{crys} = K\sin^2\varphi, \quad (8.4)$$

where φ is the total angle of deviation of a given spin from the anisotropy axis. Then the total energy of the crystalline anisotropy, summed over the entire wall, per unit area of the wall:

$$E^w_{crys} = \sum_1^N Ka \sin^2 \varphi = \int_0^\pi \frac{ad\varphi N}{\pi} K \sin^2 \varphi = \frac{a}{2} NK. \quad (8.5)$$

The total energy of the wall is given by the sum of the exchange contribution and the contribution of anisotropy $E^w = E^w_{ex} + E^w_{cry}$. Minimizing this energy by the number of spins N involved in the formation of the wall, we obtain

$$\frac{dE}{dN} = 0 \implies \frac{1}{2} aK - JS^2 \frac{\pi^2}{a^2 N^2} = 0, \quad (8.6)$$

and consequently

$$N = \pi S \sqrt{\frac{2J}{a^3 K}}. \quad (8.7)$$

Let's introduce the parameter $A = 2JS^2/a$, which is called the exchange stiffness and is a measure of the stiffness of the exchange forces when the magnetization is rotated. Then the width of the domain wall can be represented as:

$$\delta = Na = \pi \sqrt{\frac{A}{K}}. \quad (8.8)$$

It can be seen that, indeed, the exchange forces tend to stretch the domain wall, and the anisotropy energy tends to compress. The characteristic width scales of the Bloch domain walls are on the order of several tens of nanometers (for Fe$\sim 40nm$). The width of the Neel domain wall in thin films can be larger, up to $1\mu m$ due to the weakness of the uniaxial anisotropy constant.

8.2 Domains structure

8.2.1 Estimation of the domain width.

Now let's estimate the width of the magnetic domain itself. For simplicity, consider domains in the form of parallel layers. Let d be the width of the domain. It is again determined by the competition of two energies. At the edges of the magnet, a stray magnetic field emerges from it, see Fig. 8.3. To minimize these fields, and hence their energy, the domain width must be reduced. On the other hand, positive energy is associated with each domain wall, which acts, on the contrary, in the direction of reducing the number of domains and, accordingly, increasing the width of each domain. The competition of these factors stabilizes the final domain width. Let's make quantitative estimates.

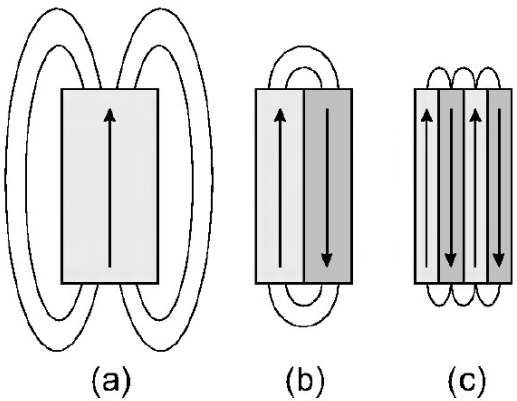

Figure 8.3: The distribution of stray fields in space. (a) A single-domain sample; (b) the same sample in a two-domain state; (c) A multi-domain state. From [5].

Substituting Na from (8.8) into the expression for the energy of the domain wall, we obtain for the energy of the surface

tension of the domain wall

$$E^w = \sigma_b = \pi\sqrt{AK} = M^2\Delta, \tag{8.9}$$

where $\Delta = \pi\sqrt{AK/M^4}$. Then the total energy of all domain walls in the sample of the width L takes the form:

$$E_b = \sigma_b \frac{L}{d} = M^2\Delta\frac{L}{d}. \tag{8.10}$$

The energy of the stray fields is of the order of magnitude

$$E_{str} = \kappa M^2 d, \tag{8.11}$$

where κ is some coefficient of the order of 1. This simple estimate is obtained as the energy of magnetic charges with a surface density of $\sigma \sim M$ distributed on the surface of the magnet $E_{str} \sim \sigma\varphi$, where the potential of the magnetic charge field is $\varphi \sim Md$.

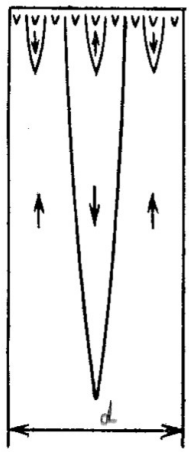

Figure 8.4: A schematic representation of the branching process of the domain at the surface of the sample.

Minimizing the total energy $E = E_b + E_{str}$ by d, we get:

$$d = \sqrt{\Delta L/\kappa}. \tag{8.12}$$

Thus, the width of the domains increases with increasing sample size as $\sqrt{L}$. But this law obviously cannot be true for arbitrarily large values of L. The width of the domains at their exit to the surface cannot exceed a certain limit value, which is determined only by the properties of the ferromagnet itself and does not depend on the shape and size of the sample. It is determined by the moment when, as d increases, it becomes thermodynamically advantageous to split the domain to a depth of the order of d. Such a moment necessarily comes with the growth of d, because the energy of the output of one domain grows as d^2, and the energy of the surface tension of the domain boundary as d. Thus, as the size of the sample increases, progressive branching of the domains should occur when they approach the surface. With sufficiently large sample sizes, branching continues until the width of the domains formed at the very surface becomes comparable to the width of the domain wall, see Fig. 8.4.

8.3 Real domain structure.

1. Crystals with strong uniaxial anisotropy demonstrate branching of domains at the surface in accordance with the theory described in the previous paragraph, see Fig. 8.5-8.6.

2. Crystals with weak uniaxial anisotropy form closing domains on the surface, see Fig. 8.7, in which the magnetization near the surface does not coincide with the easy axis, but is located parallel to the surface to minimize the energy of stray fields.

3. In crystals with non-uniaxial anisotropy the detailed domain pattern depends on the orientation of the surface with respect to the easy axes. If we move from the simplest case of a crystal surface coinciding with one of the crystal planes and containing two easy axes to a surface oriented at a large angle

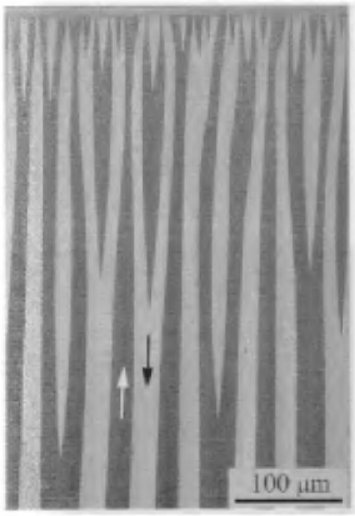

Figure 8.5: Domains on the side surface of the Co crystal. From [5].

to the crystal planes, the domain structure becomes more and more complex. Let's look at the examples.

a) Two easy axes in the plane of the surface. This situation occurs, for example, for (100)- Fe surfaces, see Fig. 8.8. The picture is easily interpreted - the magnetization in the domains is directed along one of the two easy axes lying in the plane of the surface. Locally, there is a slightly marked direction in each place of the sample due to local tensions or induced anisotropy. After complete demagnetization and subsequent magnetization, see Fig. 8.8(b), the domain structure changes somewhat, but the preferred directions remain.

b) One easy axis in the plane of the surface. This situation occurs, for example, for (110)- Fe surfaces, see Fig. 8.9. The domain structure consists of domains elongated along an easy axis.

c) A slightly misoriented surface, i.e. when the nearest easy

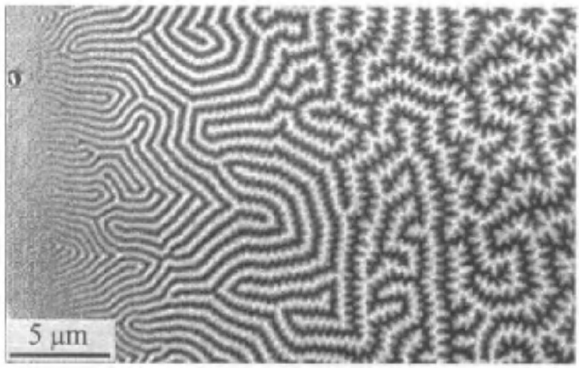

Figure 8.6: The domain structure of a wedge-shaped film of monocrystalline Co. The easy axis is directed perpendicular to the surface of the film. The film thickness increases from left to right. It can be seen that at the same time, the domain size is growing in accordance with the theory outlined above, but the degree of branching of domains at the surface is also growing. From [5].

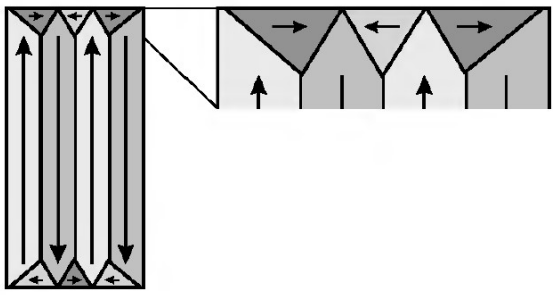

Figure 8.7: Closing domains on the crystal surface with weak uniaxial anisotropy, in which the magnetization is not parallel to the easy axis to minimize the energy of stray fields. From [5].

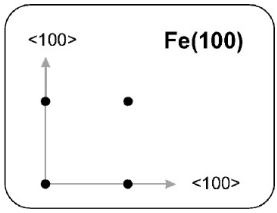

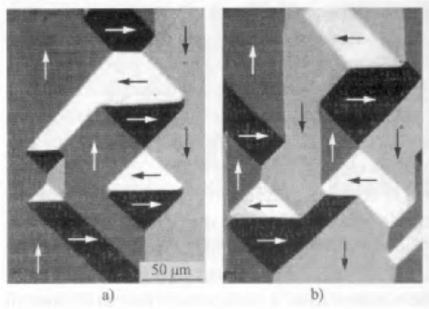

Figure 8.8: Domain structure for (100)- Fe surfaces. All domains are magnetized along one of the two easy axes lying in the plane of the surface. (b) The same sample after the next demagnetization. From [5].

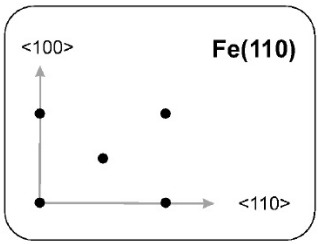

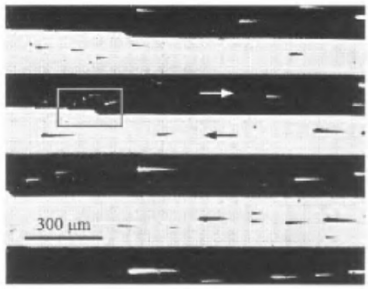

Figure 8.9: Domain structure for (110)- Fe surfaces. All domains are magnetized along a light axis lying in the plane of the surface. From [5].

axis is an angle of no more than 5° with the surface plane. The main domain structure corresponds to an ideal crystal. But "shadow domains" are superimposed on it, in which the magnetization is located along another easy axis, see Fig. 8.10.

d) Strongly misoriented surface with easy axes. In this case, the domain structure is very complex, see Fig. 8.11.

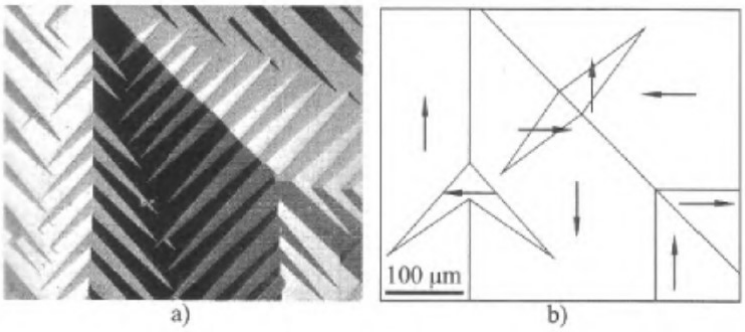

Figure 8.10: A fir tree domain structure with shadow domains on a slightly disoriented Fe surface. From [5].

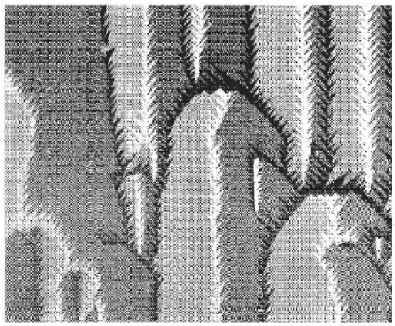

Figure 8.11: A domain structure on a strongly misoriented Fe surface. From [5].

4. The domain structure of a soft magnetic material without magnetocrystalline anisotropy, the shape of the sample is determined. It is constructed in such a way as to minimize the appearance of magnetic charges on the surface of the sample. In order for magnetic charges to disappear, the following requirements should be met:

1) $div\boldsymbol{M} = 0$ - absence of bulk magnetic charges in the sample;

2) The magnetization should be oriented parallel to the sample surfaces in order to avoid the appearance of surface charges.

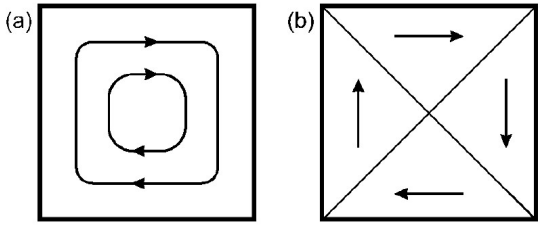

Figure 8.12: (a) The state of a square sample with continuous magnetization. (b) The Landau state with 4 domains and 90° domain walls. From [5].

Let's consider a rectangular shape sample. From Fig. 8.12(a) it can be seen that the continuous magnetization field does not satisfy all these requirements. It is divergent-free in volume, but the magnetization does not lie parallel to the entire surface of the sample. All conditions are met for the so-called Landau state, see Fig. 8.12(b). The magnetization in this state has discontinuities, which are domain walls. The magnetization is parallel to the entire surface of the sample and at the boundaries of the domains perpendicular to the surface magnetization component remains continuous, which ensures the absence of magnetic charges at these boundaries.

It is possible to formulate rules for constructing a domain structure that makes magnetic charges zero for a particle of arbitrary shape:

1) It is necessary to build circles that lie inside the sample and touch the surface at two or more points. The centers of these circles lie on the domain wall;

2) In each circle, the magnetization vector is perpendicular to the radius of contact;

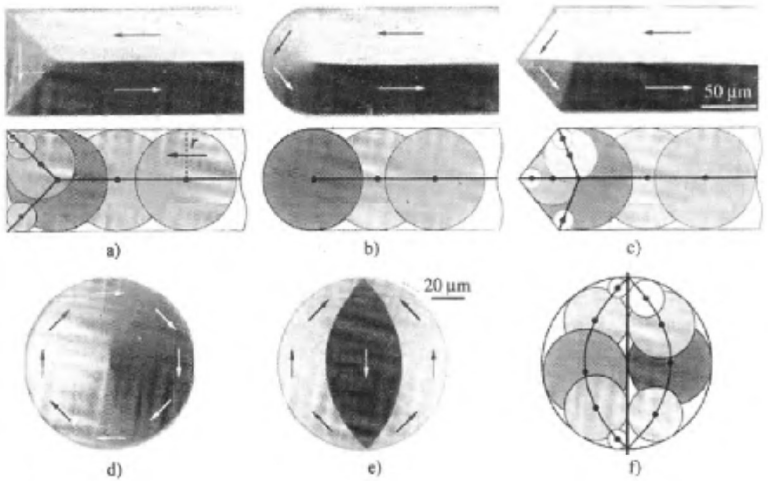

Figure 8.13: The domain structure of soft magnetic elements of various shapes. For a description of figures (a)-(c), see the text. Figures (d)-(e) correspond to the possible stable and metastable states of the disc-shaped particle. (d) - magnetic vortex; (e) domain state, which is obtained using the algorithm described in the text, but with an additional thought cut of the sample in the middle, as shown in Fig. (f). From [5].

3) If the circle touches the surface at more than two points, its center is the point of merging of the domain walls;

These rules are illustrated in Fig. 8.13(a)

4) If the circle coincides with the surface in a certain area, then the domain wall ends at its center and it serves as the central point of the domain with continuous rotation of magnetization. This rule is illustrated in Fig. 8.13(b);

5) If the sample contains a tip, then the domain wall is extended to it, see Fig.8.13(c).

The above rules lead to a state in which the energy of the stray fields is minimized. As a rule, this state is most

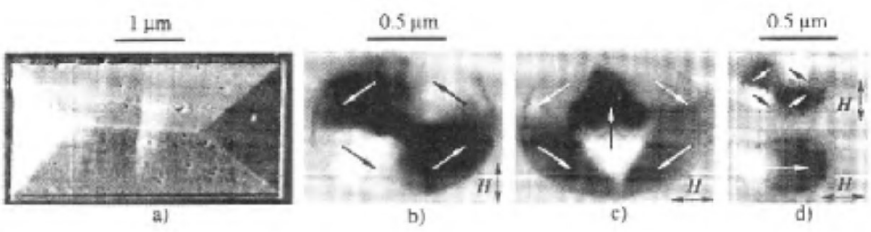

Figure 8.14: (a) A rectangular sample. (b)-(d) Elliptical Co particles of different sizes. For larger particles, a state with concentric magnetization and domain walls (b) is realized, constructed in accordance with the algorithm described in the text, or a three-domain state (c). For smaller particles, the formation of domain walls is not advantageous and a single-domain state in a parallel field or a concentric state (as metastable) in a perpendicular field is realized. From [5].

favorable for samples of sufficiently large sizes, when the loss in the energy of the formation of domain walls is compensated by the gain in minimizing the energy of stray fields. However, if the size of a magnetic particle decreases, then the formation of domain walls in it becomes unfavorable, because the energy of the stray fields is too small (recall that the energy of the domain wall grows as the sample size, and the energy of the stray fields as the square of the sample size). Therefore, when the sample size decreases, it becomes favorable for the sample to switch to a single-domain state. This process is illustrated by the experimental results shown in Fig. 8.14.

Bibliography

[1] Quantum Physics (Berkeley Physics Course, Volume 4) by Eyvind H. Wichmann, McGraw-Hill College, 1971

[2] The Feynman Lectures on Physics, Vol. 3, by Richard P. Feynman, Robert B. Leighton, Matthew Sands, Addison Wesley, 1971

[3] Albert Messiah, Quantum mechanics, volume II, Elsevier, 1961

[4] Albert Messiah, Quantum mechanics, volume I, Elsevier, 1961

[5] M. Getzlaff, Fundamentals of magnetism, Springer-Verlag, Berlin Heidelberg, 2008.

[6] The Feynman Lectures on Physics, Vol. 3, by Richard P. Feynman, Robert B. Leighton, Matthew Sands, Basic Books, 2011

[7] Е.С. Боровик, В.В. Еременко, А.С. Мильнер, Лекции по магнетизму, М:Физматлит, 2005 (in Russian).

[8] Neil W. Ashcroft, N. David Mermin, Solid State Physics, Cengage Learning, 1976

[9] M. Gibertini, M. Koperski, A. F. Morpurgo, and K. S. Novoselov, Magnetic 2D materials and heterostructures, Nature Nanotechnology **14**, 408 (2019).

[10] R. E. Peierls, Quantum Theory of Solids, Oxford University Press, 2001

[11] Vonsovsky, S. V., Magnetism, Wiley, 1974

[12] В.А. Боков, Физика магнетиков, Невский диалект, Санкт-Петербург, 2002 (in Russian).